Tampere University

Emmi Peltola

NUMERICAL AND EXPERIMENTAL EVALUATION OF ACUROS BV ALGORITHM FOR BRACHYTHERAPY

Faculty of Medicine and Health Technology
Master of Science Dissertation
Examiners: Professor Michiel Postema &
Associate Chief Physicist Jarkko Ojala
April 2022

ABSTRACT

Emmi Peltola: Numerical and Experimental Evaluation of Acuros BV Algorithm for Brachytherapy
Master of Science Dissertation
Tampere University
Master of Science Programme in Electrical Engineering
April 2022

High-dose-rate internal radiation therapy is used in the treatment of vaginal vault after surgical removal of uterine corpus. For accurate and efficient radiation therapy treatment, individual treatment-planning and accurate radiation dose calculation. Acuros BV Algorithm is a model-based dose calculation algorithm, which models the dose resulted from the brachytherapy source in inhomogeneous tissue. Historically, dose calculation has been based on dose calculation algorithms which do not take into account the tissue or applicator inhomogeneities. This master's dissertation investigates the accuracy of Acuros BV dose calculation for inhomogeneous shielded cylindrical applicator. For this investigation, dose calculations and measurements with diode and film were conducted in three different shield geometries, 90° shielding, 180° shielding, and 270° shielding. It was found that Acuros BV can be used for estimations of dose with a shielded cylindrical applicator, but a correction factor is recommended to account for the underestimation of dose exhibited by the algorithm. Acuros BV performed mostly within 10% inaccuracy limit for 180° and 270° configurations on the unshielded side of the applicator, while producing more error for the 90° shielding geometry, and results on the shielded side of the applicator.

Keywords: TG-43, Acuros BV, gynaecological brachytherapy, radiation dose simulation, radiation therapy treatment-planning, dose calculation algorithm, gynaecological tumour, brachytherapy dosimetry

The originality of this dissertation has been checked using the Turnitin OriginalityCheck service.

TIIVISTELMÄ

Emmi Peltola: Acuros BV -algoritmin numeerinen ja kokeellinen arviointi
Diplomityö
Tampereen yliopisto
Sähkötekniikan diplomi-insinööri-ohjelma
Huhtikuu 2022

Korkean annosnopeuden brakyterapiaa käytetään emättimen pohjukan hoitoon kohdun poistoleikkauksen jälkeen. Tarkkaan ja tehokkaaseen radioterapiahoitoon vaaditaan yksilöllistä hoidon suunnittelua ja tarkkaa säteilyannoksen laskentaa. Acuros BV Algoritmi on malliperusteinen annoslaskenta-algoritmi, joka mallintaa brakyterapialähteen muodostaman annoksen epähomogeenisessä kudoksessa. Historiallisesti, annoslaskenta on perustunut annoslaskenta-algoritmeille, jotka eivät huomioi kudoksen tai applikaattorin epähomogeenisyyksiä. Tässä diplomityössä tutkitaan Acuros BV -algoritmia epähomogeenistä suojattua sylinteriapplikaattoria varten. Tätä tutkimusta varten annoslaskut sekä annosmittaukset suoritettiin käyttäen diodia ja filmiä kolmelle eri suojausgeometrialle, 90° suojauksella, 180° suojauksella ja 270° suojauksella. Huomattiin, että Acuros BV:tä voidaan käyttää arvioimaan annosta suojatulle sylinteriapplikaatorille, mutta korjauskerrointa suositellaan korjaamaan algoritmin tekemää annoksen aliarviointia. Acuros BV toimii enimmäkseen 10% virherajan sisällä 180° ja 270° suojaukselle ei-suojatulla puolella applikaattoria, tuottaen enemmän virhettä 90° suojausgeometriassa sekä suojatulla puolella applikaattoria.

Avainsanat: TG-43, Acuros BV, gynekologinen brakyterapia, säteilyannoksen simulointi, sädehoidon suunnittelu, annoslaskentamalli, gynekologinen kasvain, brakyterapia dosimetria

PREFACE

I want to acknowledge Tampere University Research Services for providing me with the opportunity and materials to write my master's dissertation. I also wish to give special thanks to STUK's Senior Inspector Petri Sipilä for providing the equipment and materials needed for conducting the measurements, as well as his expertise and readiness to help in the actual measurement session and beyond it.

I wish to thank all of my supervisor for their plentiful help and guidance throughout this whole project. I thank Department Chief Physicist Eeva Boman for her help on both the practical and the theoretical aspects of the work, as well as her dedication to her field and to helping me along with my journey. Thank you for all you have taught me during the time spent working on this dissertation. I also want to thank Associate Chief Physicist Jarkko Ojala for his encouragement and assistance during my visits at the hospital, and the advice I got from him regarding my studies.

I want to thank both of my university supervisors, Professor Jari Hyttinen and Professor Michiel Postema, for their instruction regarding my master's dissertation, as well as my studies in general. Thank you, Professor Hyttinen for your encouragement and guidance throughout the project, as well as on your advice regarding postgraduate studies. Thank you, Professor Postema for pushing me to do my very best and being ready to assist me at a moment's notice. Also, thank you for the excellent talks and your invaluable counsel over the span of the semester.

Thank you also to family and friends. Your loving words, support and understanding, as well as the periodical distractions, were irreplaceable during the time spent working on this dissertation. I'm fortunate to have such dedicated people supporting me.

Tampere, April 11, 2022

Emmi Peltola

CONTENTS

LIST OF FIGURES

LIST OF SYMBOLS AND ABBREVIATIONS

Abbreviation	Description	Unit
A	activity	Bq, Ci
A_{ion}	the correction for the collection efficiency	
$C_{T,P}$	the temperature and pressure correction factor	
$\dot{D}$	2-dimensional dose rate function	
d	distance	cm
E	energy	kJ
E_{tr}	energy transferred	kJ
F	2-dimensional anisotropy function	
G_{L}	line-source approximation	
g_{L}	the radial dose function	
$\dot{K}_{\delta}$	air-kerma rate	Gy/h
L	length	cm
L_{eff}	effective length	cm
M	mass of the atom	amu
m	mass	kg
N_{A}	Avogadro's number	mol^{-1}
N_{K}	the air-kerma rate calibration factor	Gy/nC
n	the normal vector to surface	
P_{grad}	the gradient correction	
P_{ion}	the correction for collection efficiency	
Q	charge	nC
Q_{L}	leakage charge	nC
q_{p}	photon point source	
q_{scat}	photon scattering source	
r	radial distance	cm
r_0	reference distance	cm
S_{K}	air-kerma strength	$\mu Gym^2/h$, U
T	temperature	°C
$T_{1/2}$	half-life time	d
t	elapsed time	s
V	volume	cm^3
Y	Spherical harmonics function	

δ	Dirac delta function	
θ	angle	°
λ	the decay constant	s^{-1}
σ	the macroscopic atomic cross section	cm^{-1}
$\tilde{\sigma}$	the microscopic cross section	cm^2/atom
σ_t	the macroscopic total cross section	cm^{-1}
Λ	the dose-rate constant	$\mu Gym^2/hU$
ρ	material density	g/cm^3
ϕ	the spherical harmonics moments	
Ψ	the angular photon fluence	J/cm^2
$\hat{\Omega}$	direction	

AAPM	The American Association of Physicists in Medicine
ESMO	The European Society for Medical Oncology
HDR	High-dose-rate
LBTE	The Linear Boltzmann Transport Equation
LDR	Low-dose-rate
SFD	Stereotactic field diode

1. INTRODUCTION

1.1 Motivation

Internal radiation therapy, also known as brachytherapy, is used in the treatment process of gynaecologic malignancies, such as cervical and endometrial cancers. According to global cancer statistics of 2020, cervical cancer was the fourth most frequently diagnosed cancer and the fourth leading cause of cancer death in women, while uterine corpus cancer was ranked the sixth most commonly diagnosed cancer in women [1]. For safe and effective radiation treatments, an accurate model for calculating radiation dose in the patient is needed.

Treatment-planning algorithms are an important aspect of modern radiation therapy. Algorithms for dose calculation are used in treatment-planning to estimate the absorbed dose in the treatment area, as well as to estimate the risk to critical organs of the patient caused by radiation before treatment is applied. Before a dose calculation model can be approved for clinical use, it needs to be validated. In the validation process, the values obtained via dose calculation are compared against the dose measurements and known values in a standard geometry.

The purpose of this study was to conduct a model-based dose calculation algorithm validation protocol and study whether this algorithm could be implemented in clinical practice. Potentially, this validation could lead to more accurate and efficient cancer treatments than what has been achieved using conventional dose calculation methods.

1.2 Background

1.2.1 Internal Radiation Therapy as Treatment for Cancer

Brachytherapy is a form of radiation therapy, in which the radiation is given to the patient at a short distance internally. This typically involves introducing a radiation source into the body, so that radiation may be delivered to a specific area of the body. Brachytherapy treatment may be conducted by intracavitary, or interstitial means and it can be implemented as a treatment for many different types of cancers, such as prostate, cervical,

endometrial, and breast cancers. In intracavitary treatments, different target specific applicators are applied inside body cavities, while interstitial treatments involve the insertion of needles inside the target tissue, typically involving patient anaesthesia.

Historically, the first reported cases of successful brachytherapy treatments date back to the mid and late 1900s [2]. These treatments were conducted using radium as the source for radiation, and the radiation was typically delivered via an appropriate applicator, often made of silver [2].

However, because of radium's long half-life, it is not particularly useful for treatment modalities that involve use of needles [2]. For this purpose, its first daughter product, radon, which has a much shorter half-life, was implemented into clinical use. Additionally, a radon needle can be made much thinner than one made using radium because of its high specific activity. Radon needles encapsulated in steel or gold were used as internal radiation therapy particularly in the 1910s [2].

While these needles somewhat resembled modern brachytherapy seeds, it was not until after World War II that man-made radionuclides were made available for peaceful purposes, such as medical applications [2]. Specifically in Finland, the study of nuclear medicine and medical radionuclides was first launched in the 1940s [3].

Before afterloading techniques, brachytherapy had fallen out of clinicians' favour because of concerns of the personnels' safety [4]. The first remote afterloading system was introduced in 1962 [4]. These systems are devices that can remotely administer radionuclides automatically to the treatment area, providing protection to the clinician and other personnel taking part in the treatment.

Currently, nuclear medicine and modern brachytherapy are an integral part of modern medicine. Brachytherapy is used in a multitude of ways, including diagnostics, radiation therapy and nuclear imaging. Modern brachytherapy is an important aspect of highly targeted radiation therapy. During the last 40 years, afterloading techniques, image-guiding technologies, new radioisotopes, as well as faster and better computer systems have shaped brachytherapy into its modern form today [5].

Another achievement for modern brachytherapy is the development of new radioisotopes. While radon and radium are the materials of radiation sources historically, nowadays more desirable materials exist for the purposes of cancer treatment. Depending on the treatment region and amount of needed dose, different radioisotopes may be implemented into the treatment. These radioisotopes have half-life values ranging from multiple years to just a couple of days with different dose rates and emission types. Based on

the dose rate of the radioisotope, differently paced dose rate treatment modalities have likewise been developed, which will be discussed in further detail later in this chapter.

The current most commonly clinically used radioisotopes, as well as their half-lives, dose rates and common uses, are presented in Table 1. From this table, the differences between clinical radionuclides are highlighted. Noteworthy radionuclides in the scope of this study are the nuclides used in intracavitary brachytherapy, particularly Iridium-192 (Ir-192).

Table 1. Radioisotopes in common clinical use. An excerpt from [6]*. HDR referring to high-dose-rate, LDR to low-dose-rate, PDR to pulsed-dose-rate, and vLDR to very-low-dose-rate.*

Isotope	**Half-life**	**Dose rate**	**Uses**
Cobalt-60	5.26 y	HDR	Intracavitary
Cesium-131	9.7 d	vLDR	Permanent interstitial implants
Cesium-137	30 y	LDR	LDR intracavitary brachytherapy
Iodine-125	59.6 d	vLDR	Permanent interstitial implants
Iridium-192	74.2 d	HDR/PDR	HDR/PDR interstitial and intracavitary
Strontium-90	28.8 y	HDR	Plaques
Ruthenium-106	1.02 y	HDR	Plaques

Depending on the physical properties of a radioisotope, it can deliver high-dose-rate (HDR), low-dose-rate (LDR), or very-low-dose-rate brachytherapy. Often, HDR brachytherapy is most convenient for the patient because of shorter treatment times and possibly fewer complications [6]. However, most of the clinical experience in brachytherapy has been obtained using LDR implants, this treatment modality being the oldest method of brachytherapy treatment.

Another brachytherapy treatment method is the pulsed-dose-rate (PDR) brachytherapy. This modality is a relatively new one, but it has advantages such as optimisation of dose rate distribution, no need for source preparation or source inventory, as well as flexibility

between different brachytherapy treatment methods (intracavitary, interstitial, intraoperative and intraluminal) while still using the same machinery [7].

The difference between LDR and HDR brachytherapy lies within the prescribed dose rates. For LDR, this dose rate is on the order of 0.5 to 2 cGy/min, while for HDR has been classified as 20 cGy/min or higher by the International Commission on Radiation Units and Measurements [8]. PDR brachytherapy combines the physical advantages of HDR brachytherapy and the radiobiological advantages of LDR brachytherapy, using a single stepping source that produces treatment dose rates up to 3 Gy/h, pulsed typically each hour of the day [7].

1.2.2 Approaches to Gynaecologic Cancers

Gynaecologic cancers refer to all the cancer types originating from the female reproductive organs. Examples of these cancers include ovarian cancer, cervical cancer, vaginal cancer and uterine corpus cancers, i.e., endometrial cancer and uterine sarcoma. The typical application areas of gynaecological brachytherapy are uterine corpus and endometrial cancers.

When it comes to gynaecological brachytherapy, not all gynaecological cancers require the same kind of intracavitary, internal radiation therapy treatment. In the context of this work, of the two uterine corpus cancers, endometrial cancer will be awarded greater focus, given that it is more relevant to the overall scope of this thesis. Additionally, it is significantly more common than uterine sarcoma. While cervical cancer treatment does not typically include treatment via intracavitary methods, its treatment methods will also be discussed, given that in some cases this cancer may spread to the walls of the vaginal canal and require treatment via intracavitary HDR brachytherapy.

Depending on the type and location of the tumour, as well as its size, spread and metastasis (i.e., its stage), different approaches to its treatment can be taken. Typical treatment options consist of surgery, chemotherapy and/or radiation therapy. Radiation therapy options may range from external beam radiation to different types of brachytherapy. In this chapter, treatment options for different gynaecologic malignancies will be described.

As stated earlier, cervical cancer was the fourth most frequently diagnosed cancer and the fourth leading cause of cancer death in women in year 2020, while uterine corpus cancer was ranked the sixth most commonly diagnosed cancer in women [1]. Particularly in low-income and middle-income countries, the incidence and prevalence of cervical cancer is high [9]. This statistic creates a requirement for efficient and accurate treatment methods for gynaecological cancers.

Given the relatively high frequency of cervical and endometrial cancer diagnoses, preventative and precautionary measures have been implemented in many countries, particularly in high-income nations. Persistent papillomavirus infection is the most significant cause of cervical cancer and the human papillomavirus is detected in 99% of cervical tumours [10]. This is why the human papillomavirus vaccinations are an important advancement in preventing cervical cancer and why these vaccinations are included in national vaccination programmes in many countries, e.g., in Finland for school-age girls since 2013 and boys since 2020.

Another precautionary method is cervical cancer screening, which ensures the early detection of these cancers. These screenings typically consist of a human papillomavirus test, which is performed with a Papanicolaou (Pap) smear test.

The European Society for Medical Oncology (ESMO) has defined guidelines in clinical practice for the diagnosis, treatment and follow-up of cervical and endometrial cancer. According to these guidelines, for cervical cancer, the diagnosis after an abnormal cervical cytology or a positive high-risk human papillomavirus test should commence with colposcopy and biopsy or excisional procedures, such as loop electrosurgical excision and conisation (cone biopsy) [10]. Three categories of epithelial tumours of the cervix are recognised by The World Health Organization. These categories are squamous, glandular, and other epithelial tumours.

For endometrial cancer, generally, diagnosis occurs in the tumour's early stages, since abnormal uterine bleeding is the presenting symptom in 90% of cases [11]. The current trend in the investigation leading to diagnosis of endometrial cancer is toward minimally invasive exams using endometrial biopsy, vaginal ultrasound scan, as well as hysteroscopy. Similarly, the typical methods of treatment have shifted more in the direction of minimally invasive techniques [11].

Additionally, image-guidance has gone through notable developments over the last decades, which has increased the use of 3-dimensional image-guided procedures in brachytherapy [12]. Imaging modalities, such as computed tomography, magnetic resonance imaging, and ultrasound, have been successfully and rapidly utilised in the field of internal radiation therapy, giving more ability to control the radiation dose to the tumour and surrounding tissues [12].

After diagnosis of cancer and before application of any treatment, The International Federation of Gynaecology and Obstetrics encourages the use of advanced imaging modalities, such as computed tomography, magnetic resonance imaging and positron emis-

sion tomography, whenever possible [2]. Of these imaging modalities, magnetic resonance imaging is most useful for finding and assessing uterine, cervical and vaginal tumours, given its great soft-tissue resolution [2].

Cervical and endometrial cancers are staged using The International Federation of Gynaecology and Obstetrics and the Union for International Cancer Control cancer staging system, TNM classification system. In this classification system, the size of the cancer and its spread to nearby tissues, the spread to nearby lymph nodes, and the metastasis of the cancer are described. Additionally, tumour risk assessment is conducted along with classification. The treatment of the cancer is adjusted according to these parameters.

The treatment of cervical cancer may include multiple steps. These steps typically consist of surgery, chemotherapy and radiation therapy. The primary treatment modality is surgery, although depending on the stage of the cancer, surgical options may range from conisation or trachelectomy to hysterectomy with bilateral lymph node dissection [10]. For locally advanced cervical cancer, neoadjuvant chemotherapy followed by surgery or radiation therapy are typically required [10].

The standard treatment for locally advanced cervical cancer consists of external radiation therapy combined with chemotherapy [13]. This is typically followed by a brachytherapy application to increase the focal dose to the primary tumour. This standard treatment is defined in international guidelines [13].

As with cervical cancer treatment, radiotherapy and chemotherapy can be implemented into the treatment of endometrial cancer when surgery alone is not sufficient. Radiotherapy may similarly be implemented as external beam radiation and/or brachytherapy.

For endometrial cancer, adjuvant radiotherapy and/or chemotherapy is a typical treatment modality of choice [11]. External beam radiation has been proven to reduce the rate of locoregional recurrence in intermediate risk endometrial cancer, although the optimal method of adjuvant therapy has not yet been defined [11].

Radiation therapy may also be given after surgical procedures. Internal radiation therapy can be used to deliver a radiation dose directly to the vaginal vault with the purpose of preventing relapses. The vaginal vault, also called the vaginal cuff, is the main location of relapse after surgery and postoperative radiotherapy has been proven to diminish it [14].

In some rare cases, cervical or endometrial cancers may spread from the cervix and the uterus onto the vaginal walls, forming metastases. This type of secondary vaginal cancer is more common than cancer originating from the vaginal wall, which is considered one

of the rarest forms of gynaecological tumours [15]. For primary and recurrent vaginal cancer, the treatment is typically external beam radiation followed by brachytherapy [16].

Secondary vaginal cancer, or vaginal metastasis, may be treated differently than primary vaginal cancer. No single standard treatment for vaginal metastases has been established [17]. However, treatment options range from some surgical options to chemotherapy and radiotherapy, similarly to other gynaecological cancers.

1.2.3 Gynaecological Brachytherapy

Gynaecological brachytherapy is a specific treatment method, centred around treating different types of tumours presenting on the female reproductive system using internal radiation therapy. In this chapter, typical treatment methods, equipment, and materials for gynaecologic brachytherapy will be described.

For many gynaecologic malignancies, brachytherapy is a preferred treatment option, as detailed in the earlier subchapter. However, methods of delivering radiation via brachytherapy may also vary vastly on a case-to-case basis. Most often, brachytherapy is combined with external beam radiation.

Internal radiation therapy treatment may vary in the dose-rate applied. Different advantages and disadvantage lie with HDR, LDR and PDR brachytherapy treatments. Differences between LDR and HDR brachytherapy as treatment modalities have been studied and compared in relation to cervical cancer. No significant difference in overall survival rate or local recurrence between HDR and LDR techniques have been detected when it comes to treatment of patients with cervical cancer ranging from stages I through IV [18,19]. However, benefits, such as shorter treatment times and fewer complications, as described briefly in a previous subchapter, may often tip the scales in favour of HDR over LDR.

For endometrial cancer, similarly the overall survival rate seems to be the same between HDR and LDR brachytherapy [20]. However, a reduction in gastrointestinal and genitourinary toxicities without worsening of vaginal stenosis rates has been associated with the use of HDR brachytherapy over LDR brachytherapy [20].

Gynaecological brachytherapy treatment is typically given vaginally. Brachytherapy treatment for cervical cancer consists of inserting a thin applicator tube within the uterine cavity, while another part of the applicator is inserted within the vaginal cavity [13]. This procedure may be done under general or spinal anaesthesia, given that it requires the dilation of the cervical canal. To improve the dose in the target volume, the applicator

may also include needles that can be inserted into the cervix. After the applicator insertion, 3-dimensional imaging is used for the treatment-planning, in which the target and organs at risk are contoured and source positions and dwell times optimised to find optimal dose distribution. Currently, cervical brachytherapy combined with external beam radiation therapy is part of the standard treatment of locoregional recurrence of endometrial cancer [21]

For endometrial cancer, brachytherapy is commonly applied after a hysterectomy to reduce the chance of recurrence. While there is no standard adjuvant treatment method for intermediate risk endometrial cancer, benefits of external beam radiation combined with brachytherapy have been reported [11]. Both modalities are effective in treating endometrial cancer, however fewer gastrointestinal toxic effects are associated with vaginal brachytherapy than with external beam radiation therapy in high-intermediate risk cases [20]. For certain endometrial cancers without uterine risk factors, brachytherapy alone may be adequate enough as a treatment, but otherwise external beam radiotherapy should be included into the treatment [22].

1.3 Research Question

Accurate and efficient treatment-planning is a requirement for successful gynaecological brachytherapy. For this purpose, this dissertation will study the Acuros® BV algorithm (Varian Medical Systems, Palo Alto, CA, USA) for brachytherapy treatment-planning and find out whether this algorithm could be applicable for clinical use.

The research questions for this study included investigating the accuracy of Acuros BV algorithm in pre-chosen reference points in different shield geometries inside a water phantom, as well as comparison to values specified by the manufacturer. Additionally, the magnitude of error between dose calculations and dose measurements was to be identified, and the dose calculation results of Acuros BV compared with results produced with the TG-43 formalism.

1.4 Outline

In this master's dissertation, the relevant literature and theory is presented in the Introduction and Theory. In Theory, the key algorithms and their working principles are explained, in addition to basic concepts regarding the implementation of gynaecological HDR brachytherapy. In Methods and Materials, the experiment setup is presented and

explained, and the protocol for the validation of the algorithm defined. Results are presented in Results and their meaning and validity discussed in Discussion. In Conclusions, the central information obtained from this study will be summarised.

2. THEORY

2.1 Treatment-Planning

Conventional treatment-planning for the clinical implementation of brachytherapy treatments has been based on evaluation of dose distributions in standard geometries. Additionally, dose distributions have traditionally been studied in water.

Modern treatment-planning, on the other hand, is based in evaluating dose distributions in healthy tissues and the use of imaging modalities for the evaluation of the tumour, typically with computed tomography or magnetic resonance imaging. Dose calculation, however, is still largely implemented using water instead of tissue.

For HDR brachytherapy treatments, treatment-planning begins with patient preparation and the placement of applicators, catheters or needles to the treatment area [8]. Different methods of guidance can be implemented. For instance, gynaecologic applicators are placed typically using palpation and visual inspection, while in other cases image-guidance, such as ultrasound, may be used [8].

After the placement of the applicator, the patient is simulated using an isocentric X-ray unit or a simulator [8]. More often nowadays, 3-dimensional methods, such as computed tomography or magnetic resonance imaging, are utilised. A marker wire, which are used for the determination of the length of the applicator and/or catheter used in treatment, can be inserted all the way to the closed end of the applicator assembly for easier localisation. In traditional, 2-dimensional method, orthogonal radiographs are obtained for the localisation of the applicator and marker wire, which enable the clinician to accurately plan the treatment segment and dwell times. Additionally, the length of the catheter is determined [8].

Once simulation data is obtained, computer planning may begin, where patient and simulation data are loaded into the treatment-planning software for the optimisation of the brachytherapy treatment [8]. Nowadays, 3-dimensional imaging modalities are used for the creation of treatment-plans. Sources or applicators implemented on the treatment-planning software can be placed on the image of the patient to create treatment plans with individual patient specifications.

Particularly for cervical cancer treatment, 3-dimensional brachytherapy technique has been reported to increase local control and reduce toxicity when compared to 2-dimensional techniques [23]. When comparing the two techniques in relation to endometrial

cancer, it has been reported that 3-dimensional treatment-planning could offer more appropriate dose to the target tissues while reducing dose to organs at risk [24].

Treatment-planning may be conducted via forward or inverse planning. The key differences between these treatment optimisation methods are the changes in the responsibilities of the clinician and the treatment-planning software, as well as the order of the calculation of treatment parameters. For instance, forward planning begins with the setting of dwell times and continues on to calculate dose distribution, while inverse planning begins at the setting of desired dose distribution, based on which the dwell times are calculated. Additionally, a reference line or planning target volume is required for successful inverse planning optimisation.

For HDR brachytherapy, benefits, such as better plan optimisation and higher radiation doses to target tissues, have been associated with inverse planning for cervical cancer treatments [25, 26]. For endometrial and vaginal cancer treatments, the same has been noticed particularly when using a multichannel applicator [27, 28].

2.2 Dose Calculation Algorithms

Another aspect to consider when working on treatment-planning, are the different algorithms that may be utilised for accurate and efficient dose calculation for brachytherapy treatments. Treatment-planning algorithms are used for radiation dose calculations to deliver higher doses of radiation to target organ, while reducing dose to surrounding tissues and organs at risk. They can be classified based on their working principles, and generally these algorithms are divided into factor-based algorithms and model-based algorithms [29].

With factor-based algorithms, also known as correction-based or measurement-based algorithms, the calculations begin at the measurement of the absorbed dose in a water phantom [29, 30]. A rectangular beam incident, typically on the surface of the phantom, is used to create the absorbed dose. The input data is parameterised into distributions of the absorbed dose as functions and then applied to account for the difference between the phantom setup and the patient-specific conditions, such as tissue inhomogeneities [29, 30]. Examples of factor-based algorithms are the Clarkson algorithm and the TG-43 formalism.

In other words, the factor-based algorithm corrects the calculated absorbed-dose distribution based on its input parameters. Model-based algorithms, on the other hand, directly compute the absorbed dose per energy fluence in the patient [29]. These models

typically consist of two parts, the part that models the beam and represents the fluence distribution, as well as the part that models the patient, typically based on a tomographic representation of the patient [29].

Convolution-superposition algorithms are an example of a model-based approach to dose calculation. Currently, convolution-superposition algorithms are the overall most commonly utilised algorithms for treatment-planning in clinical practice [31].

In the following subchapters, the TG-43 algorithm and Acuros BV will be introduced. Additionally, their basic working principles will be explained.

2.2.1 TG-43 Algorithm

For gynaecologic brachytherapy dose calculation, the current international standard is the TG-43 formalism, first published in 1995 and later on updated in 2004. Since the inner pelvic area is quite water equivalent, this model is, in most cases, a reasonable option for treatment-planning in this specific area of the body. As is, this formalism is the most widely used one when it comes to gynaecological brachytherapy.

In addition to assuming the water medium, the TG-43 formalism also assumes homogeneity, which creates error when radiation treatment is applied to inhomogeneous matter. Other limitations of the TG-43 formalism include assumption of perfect source superposition and full scatter conditions, i.e., an infinite medium. When compared to Monte Carlo dose calculation methods, the weaknesses associated with TG-43 formalism, such as the aforementioned ones, have been reported previously [32, 33].

The American Association of Physicists in Medicine (AAPM) has defined the TG-43 protocol using five definitions for the relevant concepts [34]. A brachytherapy source has been defined as any encapsulated radioactive material that can be used for brachytherapy treatments, with no restrictions to its size or symmetry. Additionally, a point source was defined as a dosimetric approximation in which radioactivity is assumed to subtend a dimensionless point with a dose distribution assumed to be spherically symmetric at a given radial distance r. By diving one with the radial distance squared, the inverse square law can be calculated for the interpolation between tabulated transverse-plane dose-rate values. For a cylindrically symmetric source, the transverse-plane is the plane perpendicular to the longitudinal axis of the source and bisects the radioactivity distribution [34].

A line source is defined as a dosimetric approximation whereby radioactivity is assumed to be uniformly distributed along a 1-dimensional line-segment with an active length L [34]. This approximation does not accurately characterise radioactivity distribution within

an actual source, but for the characterisation of the influence of inverse square law on a source's dose distribution for the purposes of interpolating between or extrapolating beyond tabulated TG-43 parameters within clinical brachytherapy treatment-planning systems. A seed is a cylindrical brachytherapy source with active length L, or effective length, L_{eff}, less than or equal to 0.5 cm in length [34].

The general 2-dimensional formula for the TG-43 protocol

$$\dot{D}(r,\theta) = S_{\mathrm{K}} \cdot \Lambda \cdot \frac{G_{\mathrm{L}}(r,\theta)}{G_{\mathrm{L}}(\mathrm{r}_0,\theta_0)} \cdot g_L(\mathrm{r}) \cdot F(r,\theta), \qquad (1)$$

where r is the distance from the center of the active source to the point of interest, r_0 the reference distance (1 cm in this protocol), θ the polar angle, and θ_0 the source transverse plane (90° or π/2 radians) is also given by the AAPM [34]. Additionally, constants and functions included in Equation 1 that the TG-43 protocol calculates, are Λ, the dose-rate constant, g_L, the radial dose function, and F, the 2-dimensional anisotropy function.

2.2.2 Acuros BV Algorithm

To begin solving limitations presented by factor-based dose calculation algorithms, such as limited scatter conditions, different methods may be undertaken. A great option may be moving from factor-based algorithms to model-based ones, which indeed also model the scatter conditions. Particularly for cervical cancer brachytherapy treatments using intracavitary shielded applicators, model-based dose calculation could be beneficial [35]. This is because of clinically meaningful differences to dosimetric parameters of the organs at risk that have been witnessed when comparing to predictions achieved with the use of the TG-43 formalism [35].

Options for solving the scatter conditions include stochastic and deterministic methods, as well as their combinations. An example of the stochastic method is the Monte Carlo-based treatment-planning, which is considered the gold standard for brachytherapy dosimetry, despite not having been widely implemented for any software for brachytherapy treatment-planning [36]. It is considered the most efficient and consistent method of radiotherapy dose calculation, although no Monte Carlo calculation can be considered fully free of errors, similar to other calculation algorithms [37]. A noteworthy limitation to the use of Monte Carlo methods, however, is that calculation via this method may be quite slow when in comparison to other calculation methods [31].

Another option to tackle the problem of scatter conditions are the deterministic methods, such as the grid-based linear Boltzmann transport equation (LBTE). The LBTE is the

governing equation describing macroscopic behaviours of ionising radiation as it passes through and interacts with matter. Grid-based LBTE solvers have been shown to produce dose calculations comparable to Monte Carlo methods for external photon beam radiation and their use is recommended particularly when noteworthy heterogeneities are present [38].

The Acuros BV algorithm is an implementation of the grid-based LBTE method. This method is non-stochastic and more efficient than typical Monte Carlo based methods. According to the manufacturer, it was developed for providing accurate and rapid dose calculations for HDR and PDR brachytherapy treatments. Unlike TG-43, Acuros BV also takes into consideration the scatter conditions, such as the applicator and patient heterogeneities. The governing equations of this dose calculation algorithm will be discussed in further detail later in this chapter.

Acuros BV algorithm has previously been held in dosimetric comparison with the standardised TG-43 algorithm, e.g., in relation to interstitial HDR brachytherapy treatment for breast cancer patients, during which dosimetry calculations were performed [39]. Based on the results of this comparison, it seems that the TG-43 formalism overestimates the radiation dose to various volumes of interest, while Acuros BV gives better accuracy by taking into consideration the catheter of the source and tissue inhomogeneity [39].

Treatment-planning systems that utilise Monte Carlo calculations for HDR brachytherapy have been validated and studied for clinical use, also [40, 41]. As stated previously, Monte Carlo methods are considered the gold standard of dose calculation. When compared to Monte Carlo methods for dose calculation, it has been reported that Acuros BV retains an accuracy comparable to Monte Carlo simulation, providing improved accuracy [33].

Given that treatment-planning is an essential part of modern brachytherapy, many studies with similar interests as in this dissertation have also been conducted previously. For instance, Acuros XB algorithm, an advanced dose calculation algorithm, which, similarly to Acuros BV, calculates the dose via the LBTE, has been studied [42]. This algorithm has been validated for photon dose calculation in external radiation therapy and was declared satisfactory for both conventional photon beams as well as for flattening filter free beams of new generation linacs [42]. Studies with similar interests as this one will be considered also later on in study.

As discussed earlier in this dissertation, Acuros BV calculates dose distributions through solving the LBTE. The working principle as well as the governing equations for of this

algorithm are described in the reference guide provided by the manufacturer of this algorithm. This form of the LBTE is the static, or time-independent, form, where volume is V and surface is δV. In this form

$$\hat{\Omega} \cdot \vec{\nabla}\Psi + \sigma_t \Psi = q_{\text{scat}} + \sum_{\text{p}=1}^{\text{p}} \frac{q_{\text{p}}}{4\pi} \delta(\vec{r} - \vec{r}_{\text{p}}), \tag{2}$$

and

$$\Psi = 0, \vec{r} \in \delta V, \hat{\Omega} \cdot \vec{n} < 0, \tag{3}$$

direction is symbolised as $\hat{\Omega}$, Ψ is the angular photon fluence, q_{scat} photon scattering source, q_{p} photon point source, $\delta(\vec{r} - \vec{r}_{\text{p}})$ Dirac delta function between point source location and position, $\vec{r}$ is function of position, σ_{t} the macroscopic total cross section, and $\vec{n}$ the normal vector to surface [38].

The first term of the right-hand side of Equation 2 is the scattering source, while the second term is the source from the prescribed brachytherapy point sources. In addition, the scattering source is the function of the angular fluence

$$q_{\text{scat}}(\vec{r}, E, \hat{\Omega}) = \int_0^{\infty} \int_{4\pi} \sigma_{\text{s}}(\vec{r}, E' \to E, \hat{\Omega} \cdot \hat{\Omega}') \Psi(\vec{r}, E', \hat{\Omega}') \text{d}\hat{\Omega}' \text{d}E', \tag{4}$$

where $\sigma_{\text{s}}(\vec{r}, E' \to E, \hat{\Omega} \cdot \hat{\Omega}')$ is the macroscopic differential scatter cross section, in which E is energy. For Ir-192 sources, photon scattering is anisotropic. In this case, the scattering source becomes

$$q_{\text{scat}}(\vec{r}, E, \widehat{\Omega}) = \sum_{l=1}^{L} \sum_{m=-l}^{l} \int_0^{\infty} \sigma_{s,l}(\vec{r}, E' \to E) \phi_{l,m}(\vec{r}, E') Y_{l,m}(\widehat{\Omega}) \text{d}E', \tag{5}$$

where $\phi_{l,m}(\vec{r}, E')$ is the spherical harmonics moments and $Y_{l,m}(\widehat{\Omega})$ the spherical harmonics functions. In addition, l and m represent the angular indices.

In addition to the static form of the LBTE, Acuros BV employs other methods for obtaining the solution. These methods are energy discretisation, point source representation, angular discretisation, spatial discretisation, and fluence to dose conversion.

Acuros BV also takes into account the relevant material properties and brachytherapy sources. For material properties, this is based on the calculation of macroscopic atomic cross sections, composed of microscopic cross section for a given reaction $\tilde{\sigma}$ and the mass density of the material ρ. Meaning

$$\sigma = \frac{N_A \rho}{M} \tilde{\sigma}, \quad (6)$$

in which M is the mass of the atom and N_A is Avogadro's number. The unit for this value is cm^{-1}. For Ir-192 sources, Acuros BV uses cross sections produced by a coupled electron-photon cross section generating code, which includes all photon interactions with the exception of Rayleigh scatter.

For the brachytherapy sources used in treatment, each source supported by Acuros BV algorithm is modelled as an effective source that consists of one, or more point sources. These sources represent the energy and angular dependent photon intensity exiting the source surface.

2.3 Implementation of Treatment

2.3.1 Calibration and Specification

After treatment-planning, aspects regarding the implementation of the brachytherapy treatment must be considered, also. This phase may include methods of dose calculation via different methods for varying purposes, often related to the safety of clinicians and patients, as well as the accuracy of the treatment to be implemented.

The calculation of radiation dose simply refers to the estimation of radioactive radiation in a certain environment. For instance, radiation calculation can be calculated for a certain time period, e.g., in the case of annual radiation dose, or perhaps for personnel working in close quarters to radiation sources for the duration of the exposure to radiation. Dose calculation is also needed for the determination of the radiation dose delivered to a patient as a treatment modality, i.e., the dose absorbed by the patient.

Radiation dose is a value used to quantify the amount of exposure to radiation. For the results to be useful for a physicist or a clinician, knowledge of the radiation dose alone is not typically enough. Instead, quantities, such as absorbed dose, effective dose, or equivalent dose may need to be determined.

While absorbed dose refers to the amount of energy deposited to matter by radiation, effective dose and equivalent dose are measures are specifically created for the purposes of radiobiological protection. Effective dose is the calculated radiation dose received by the whole body, while equivalent dose is the radiation dose calculated for individual organs and it is based on the absorbed dose to that specific organ.

Before actual treatment, other relevant parameters are typically required, as well. For brachytherapy treatments, the calibration of the radiation sources needs to be conducted [8]. This calibration consists of brachytherapy source strength specification, as well as exposure rate calibration. The source strength specification can be achieved in several different ways, including via the activity of the source, the exposure rate at a specified distance, the equivalent mass of radium, or apparent activity. Nowadays, however, the AAPM recommends air-kerma strength for the specification of brachytherapy sources [8]. This method will be discussed shortly.

Exposure rate calibration, on the other hand, can be achieved by following the standards established by the National Institute of Standards and Technology [8]. Open-air measurements or well-type ion chambers should be utilised. For Ir-192 sources, well-type ionisation chamber is considered the working standard [8].

Kerma K is the measure of initial kinetic energy that is transferred to matter as a result of ionising radiation. It is also an acronym for “kinetic energy released per unit mass” and its unit is gray (Gy). This can be represented as

$$K = \frac{\mathrm{d}E_{\mathrm{tr}}}{\mathrm{d}m}, \tag{7}$$

where E_{tr} is the energy transferred and m mass. Despite sharing similarities, such as the same unit, kerma should not be confused with absorbed dose. While at lower energies the values of kerma and absorbed dose may be quite equal, at higher energies kerma is considerably higher.

For calibration, the activity and the half-life time of the source need to be known, as well. The activity of the source

$$A = A_0 \mathrm{e}^{-\lambda t}, \tag{8}$$

where A_0 is the initial activity, λ the decay constant, and t the elapsed time should be calculated [43]. A typical unit for activity is becquerel (Bq). The half-life time

$$T_{1/2} = \frac{\ln(2)}{\lambda}, \tag{9}$$

where $T_{1/2}$ is the half-life time, is also needed [43]. Typically, this value is known, since it is specific for each radioisotope.

Based on these equations, the conversion factor between air-kerma and activity can be calculated for source calibration. Based on the activity of the radiation source and the conversion factor, air-kerma rate can be calculated.

Air-kerma rate $\dot{K}_\delta(d)$ is the rate of kerma in air per hour. This value is usually inferred from transverse-plane air-kerma rate measurements that are performed in a free-air geometry at distances large in relation to the maximum linear dimensions of the detector and source [34]. Air-kerma rate

$$\dot{K}_\delta(d) = (\Delta Q - \Delta Q_\mathrm{L}) N_\mathrm{K} C_{T,P} P_\mathrm{ion} A_\mathrm{ion} P_\mathrm{grad}, \quad (10)$$

in which $(\Delta Q - \Delta Q_\mathrm{L})$ is the collected charge in the span of time with the leakage charge subtracted, N_K is the air-kerma rate calibration factor, $C_{T,P}$ the temperature and pressure correction factor, P_ion the correction for collection efficiency, A_ion the correction for the collection efficiency at the time of calibration, and P_grad the gradient correction [44]. Additionally, air-kerma rate needs to typically be converted from seconds to hours for the correct unit of Gy/h.

The air-kerma strength is the product of air-kerma rate in vacuum and the square of the distance d of the calibration point from the source center along the perpendicular bisector. The δ represents the photon energy cutoff. The air-kerma strength's

$$S_\mathrm{K} = \dot{K}_\delta(d) d^2, \quad (11)$$

recommended unit is μGym²/h [34]. For convenience, the unit is often denoted by the symbol U.

2.3.2 Applicators

Given the nature of brachytherapy as a treatment modality, different applicators are usually needed for the delivery of the radiation dose. Gynaecologic cancers can be treated via interstitial or intracavitary brachytherapy, both of which typically requiring an applicator. The applicator can be used either for the placement of a radioactive seed, or as a sheath for a catheter containing radioactive sources.

Applicator geometries range from fixed to variable and customisable, while applicator shapes depend largely on the type of the treatment. Applicators may be cone, cylinder, tandem or ovoid shaped, or even custom-built for a particular purpose. With varying geometries and shapes, it becomes possible to alter the radiation dose to the patient, as well as the size and shape of the radiation field.

Applicators may be designed with either intracavitary or interstitial brachytherapy in mind, or the treatment of cervical or endometrial cancers. Based on these selections, gynaecologic applicators are typically cylindrical or ovoid-shaped, with options to adapt the applicators to fit a certain anatomy, or to use it for placement of radioactive seeds. Each

tumour type requires its own applicator, but here only the relevant applicator geometries will be introduced.

In HDR brachytherapy for cervical cancer, tandem ovoid applicators and tandem ring applicators are the most commonly used applicator types [45]. Different advantages are associated with these applicator types, mainly various size and configuration options for tandem ovoid applicators and different loading positions and repeatability for tandem ring applicators [45]. These applicators consist of a tandem, as well as ovoids or a ring. The tandem is inserted into the cervix, while needles guided through ovoids/ring may be used for implementation of interstitial brachytherapy treatment to the cervix. Examples of these applicators are presented in Figure 1.

Figure 1. *Standard gynaecological applicators. On top, is a tandem ovoid applicator, while on the bottom, is a tandem ring applicator. The length of the tandem ovoid applicator is approximately 30 cm with options to vary the dimensions, while the tandem ring applicator is slightly shorter, similarly with options to vary dimensions, such as the diameter of the ring. Images courtesy of Elekta.*

Although rare, gynaecological applicators can also contain shielding, which can be configured to fit the needs of the individual patient. These cylindrical vaginal applicators are designed for the radiation of the vaginal wall and/or vaginal vault, and can be configured using metal pieces to reduce radiation, as well as plastic pieces to allow it for target

volumes. This enables the clinician to easily alter the direction and the area of the curative radiation dose, preserving some of the healthy tissues from excess radiation. For instance, the bladder or rectum may be spared from unneeded radiation by implementing shielding.

Shielded applicators are particularly useful when the patient has previously received radiation to the general treatment area, and the total amount of radiation to the tissues needs to be reduced. With shielding, the accuracy and precision of the treatment can potentially be increased.

Typically, the applicator may be configured in four different ways; 90°, 180°, 270°, or 2×90° shielded (shielded on opposing sides). Different configuration options can be viewed in Figure 2. The usual materials that the applicator/catheter is made of include plastic, e.g., acrylic plastic, while the shielding is made of metal, e.g., lead, tungsten alloy, or stainless steel. It has been reported, however, that in shielded cylindrical applicators stainless steel may be ineffective as a shield material [46].

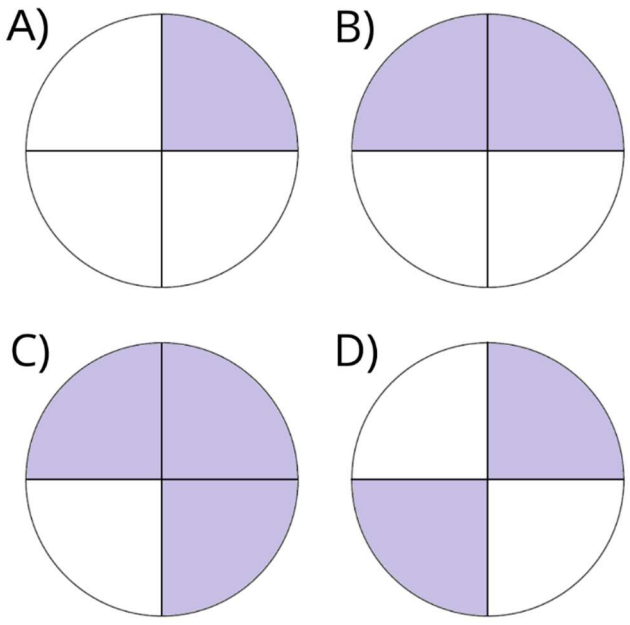

Figure 2. *Possible configurations for cylindrical shielded applicators. Shielded quarters are indicated in color. It is to be noted that during treatment, these shield geometries are surrounded by the cylindrical applicator, as well. A) 90°, B) 180°, C) 270°, and D) 2×90°.*

Applicators may vary also in the number of channels. Typically, cylindrical vaginal applicators for intracavitary brachytherapy are either singe-channel or multichannel applicators. For the treatment of vaginal cancer, benefits in using multichannel vaginal cylinder applicator as opposed to a single-channel applicator in brachytherapy treatments have also been proposed [16]. Similarly, for endometrial cancer, advantages have been observed using multichannel applicators combined with inverse planning over single-channel cylinders [27].

3. METHODS AND MATERIALS

3.1 Experiment Setup and Calibration

For the validation process introduced in this study, different devices, software, as well as equipment were required. These requirements, as well as procedures implemented before dose calculations and measurements, will be described in this subchapter.

For dose calculations, BrachyVision™ (Varian Medical Systems, Palo Alto, CA, USA) was used, with which results of doses in pre-set reference points could be obtained using the TG-43 formalism, as well as Acuros BV algorithm. BrachyVision, a 3-dimensional treatment-planning system, was used for treatment-planning, as well as in the implementation of the treatment plan during the measurement session. Using this software, a measurement setup in a water phantom was built and differently sized applicators were inserted into the phantom. Radiation doses were calculated in different reference points for different shield geometries.

The calculations and measurements of dose for Acuros BV validation were conducted Tampere University Hospital in Radius Building. For this validation procedure, three different configurations implemented with a cylindrical gynaecological applicator were studied. These configurations were 90°, 180°, and 270° shielding. The premises for calculations and measurements, as well as all equipment needed for the validation process were provided by Tampere University Hospital and the Radiation and Nuclear Safety Authority (STUK).

The applicator chosen for the validation process belonged to a shielded applicator set, GM11004380 Shielded Applicator Set (Varian Medical Systems, Palo Alto, CA, USA), which included applicators with diameters of 20, 23, 26, 30, and 35 m. According to the manufacturer, this applicator set is intended for HDR intracavitary vaginal, vaginal stump, and rectal brachytherapy treatments, where partial shielding is needed. The shielding material is tungsten alloy, and the applicators are ethylene oxide sterilisable. The shielded applicator set used for the measurements can be viewed in Figure 3.

Figure 3. *Shielded applicator set used in dose measurements. This applicator set included five applicators with different diameters, as well as quarter cylinders to be placed inside the applicator to implement shielding. The applicators were approximately 15 cm in length.*

The applicator chosen from this set had a diameter of 30 mm and it was set to three different configurations using tungsten alloy and acrylic plastic quarter-cylinder pieces. These configurations were 90°, 180° and 270° shielded, as mentioned. The fourth possible configuration, 2×90° tungsten alloy pieces set in a butterfly-esque shape, presented earlier in Figure 2 of this work, was not used in the measurement session. This is since the 2×90° shielding configuration is rarely used in clinical settings, and it was deemed that validation can be conducted accurately enough using the three remaining configurations.

The measurements were performed at the hospital's brachytherapy room, where radiation treatment could be implemented remotely from the adjacent treatment-planning room. Afterloader system BRAVOS™ (Varian Medical Systems, Palo Alto, CA, USA) was utilised for the application of the dose. The same treatment plan and treatment-planning room were utilised for dose calculations, as well.

The measurements were conducted using a water phantom, constructed of a 30 cm × 30 cm × 30 cm PMMA container that was filled with tap water. The applicator was submerged into the water from the open top of the cube and held in place on a horizontal stand, the applicator's distal end pointed towards the floor. Using the built-in measure of the stand, the applicator was located so that its surface was situated at 120 mm in horizontal direction.

Next to the applicator, a measurement device was similarly submerged and adjusted to an appropriate distance by using the built-in measure. The measurement device was pointed horizontally towards the applicator and submerged so that a distance of 30 mm

remained from its location to the distal end of the applicator in vertical direction. An example of this measurement setup can be viewed in Figure 4.

Figure 4. *Pictured in this figure is the experiment setup. The applicator was submerged into a 30 cm × 30 cm × 30 cm container filled with tap water, and the detector was placed on its side with the shielding rotated appropriately for each measurement.*

Dose measurements were performed with four alternative methods, using three types of detectors, as well as dosimetry film. Of the three detectors, one was chosen to be used for the eventual comparison between calculations and measurements, in addition to film.

These measurement devices were DEB050 stereotactic field diode (SFD) (Scanditronix Medical AB, Vislanda, Sweden), RAZOR™ Detector (Razor) (IBA Dosimetry, Schwarzenbruck, Germany), PTW-60019 microDiamond (PTW) (PTW Freiburg, Breisgau, Germany), and Gafchromic™ EBT3 dosimetry film (Ashland Global Holdings Inc., Wilmington, DE, USA). After testing, it was determined that the SFD was a good choice for conducting the validation process, since the initial readings of doses seemed more accurate than those achieved with the Razor detector. Additionally, the SFD was more convenient for multiple dose measurements, given that it does not require pre-radiation like the PTW.

The radiation source used for the measurement session was Ir-192, which was briefly introduced in this master's dissertation in Table 1. The total radioactivity, or the source strength, of the Ir-192 source was 511.85 GBq (13.88 Ci), as specified in the manufacturer's certificate. For HDR brachytherapy, Ir-192 is the best choice for source of radiation, given its higher specific activity and lower photon energy [8].

The treatment device and the radiation source were also calibrated during measurement session. This was achieved by using two different well chambers, PTW well chamber

TW33005 sno 122130 (PTW Freiburg, Breisgau, Germany) and HDR 1000 Plus well chamber sno A990881 (Standard Imaging Inc, Middleton, WI, USA).

For the calibration, air-kerma strength of the radiation source was calculated using Equation 8 and Equation 9 introduced earlier in this work. Using these formulae with elapsed time t = 54.6 d and half-life time for Ir-192 source being $T_{1/2}$ = 73.83 d as starting values, a conversion factor was obtained. This value was used for the calculation of air-kerma rate by multiplying it with the conversion factor between air-kerma and activity [mGy/Cih] and the activity of the source, which was 13.88 Ci.

During the measurement session, temperature T was 21.2°C and air-pressure P was 99.76 kPa in the brachytherapy treatment room. Correction factors $C_{T,P}$ for temperature and pressure for the well chambers were 1.020 (at 20°C) for PTW well chamber and 1.013 (at 22°C) for HDR 1000 Plus well chamber, according to the manufacturer.

The calibration was continued via measurements taken with these two well chambers introduced in this subchapter. Multiple measurements were taken using these well chambers of which the maximum dose was selected to be used for calibration. Using Equation 10, values for air-kerma rate were obtained.

To conclude calibration, these air-kerma rate values were then compared to the one calculated based on the activity that the radiation source manufacturer had specified. The difference was concluded to be within acceptable inaccuracy limits, and thus the Acuros BV validation protocol was begun.

3.2 Acuros BV Validation Protocol

To validate the Acuros BV in a standard geometry given by the manufacturer, the validation procedures were followed to ensure successful installation and fulfilment of required manufacturer specifications. This was done by following the provided test procedure within the Installation Product Acceptance (Varian Medical Systems, Palo Alto, CA, USA).

This test procedure included the creation of a TG-43 dose calculation test plan, which was then imported for Acuros BV dose calculation test. A dose matrix was set up as indicated in the test procedure and the inhomogeneity corrected dose was calculated with calculation and reporting medium set as water. The values retrieved from the report of this calculation were then compared with the provided table of results with a 2% inaccuracy limit.

In addition to validation of Acuros BV in a standard geometry, the algorithm was validated in known reference points via comparison of dose calculations and dose measurements.

The same treatment plan was created and used for both dose measurements and dose calculations. Initially, multiple dose calculations for applicators with diameters ranging from 20 mm to 35 mm and all four possible shielding configurations were created.

The applicator with the diameter of 30 mm was chosen for the dose calculations and measurements performed for this study. This applicator was part of a set of shielded applicators and could be set to different configurations using quarter-cylinder and half-cylinder pieces.

For the calculations, the applicator could be chosen from the content library, where cylindrical solid shielded applicators could be selected based on their shield configuration and diameter. Applicators with 30 mm diameter and shielding configurations of 90°, 180°, and 270° were selected for calculations.

Treatment plans for each shield configuration were generated, with treatment technique being interstitial and dose per fraction 2.00 Gy. A water phantom was selected to be used during the calculations and in each plan the correctly shielded solid applicator was inserted into the phantom. The applicator was placed in the middle of the phantom, the distal end reaching the depth of 10.50 cm into the phantom.

After the placement of the applicators, a probe with 10 sources was added into the applicators. The first and last source positions of this probe were 0.1 cm and 5.0 cm and the distances between the sources were set as equal. Additionally, the dwell times needed to be set up similarly to the measurement session. These dwell times are given in Table 2.

Table 2. Dwell times for the calculations. Presented also in the table are the positions for each source in centimetres with time in seconds.

Position [cm]	Nominal time [s]	Actual time [s]
159.90	9.00	8.35
159.40	8.40	7.79
158.90	7.40	6.86
158.40	6.10	5.66
157.90	4.70	4.36
157.40	4.30	3.99
156.90	5.00	4.64
156.40	6.40	5.94
155.90	7.60	7.05
155.40	8.60	7.98

Reference points for the calculation of dosage in each point were created. Eight reference points were created and placed on the unshielded side of the applicator and four points on the opposite, on shielded side. The distances from applicator surface were 0, 1, 5, 10, 20, 30, and 50 mm on the unshielded side, and 0, 1, 5, and 10 mm on the shielded side. Additionally, twenty reference points were created to be placed on the surface of the applicator with 18° distance between each point. These reference points and their locations, as well as the sources, can be viewed in Figure 5.

Two treatment plans without applicator or shielding were created with the same reference points, as well. This was to conduct a comparison of Acuros BV and TG-43 formalism, given that the TG-43 formalism does not take into account any scatter conditions, i.e., applicator or shielding materials.

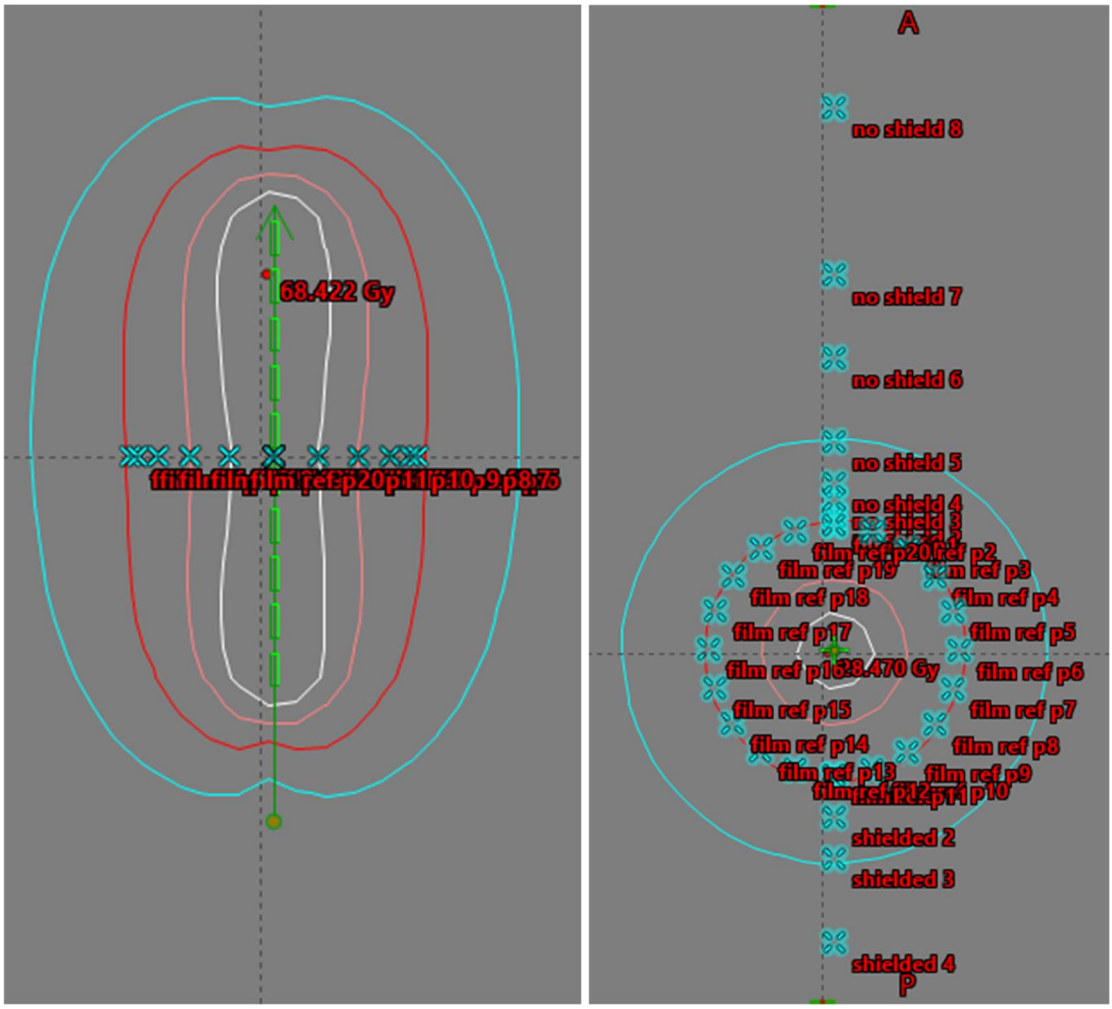

Figure 5. *The locations of the reference points without applicator inserted, only sources. Sources are indicated in green, while reference points are marked as blue crosses with their names in red.*

After the creation and placement of the reference points, dose calculations were initiated. Model-based dose calculation could be selected after first conducting factor-based calculation, i.e., the TG-43 formalism. The calculated radiation doses could be viewed by printing the brief report of the treatment plan.

The dose measurement session began with the validation of the accuracy of the treatment device and the radiation source. This was achieved via calibration, which was described earlier in this chapter.

Measurements at the reference points were taken from both the unshielded and shielded sides of the applicator by manually moving the detector on the stand. Given that the measurement session partially included testing out different detectors and methods, varying reference points were chosen and more added later on, in some cases. The overall methodology was similar to dose calculations, however.

The first round of measurements was conducted using the SFD with the applicator 180° shielded. For these measurements, the applicator was submerged into the water phantom as described earlier in this work and radiation was applied remotely from the control room. The afterloader was manually engaged for each round of radiation by initiating the Last Man Out sequence. The recorded doses from this configuration were written down by hand after each round of radiation for each reference point.

After the first measurements, other measurement devices were tested using the same 180° shield configuration. For these test measurements, the PTW and Razor were used, before proceeding onto 90° and 270° shielding configurations, which were measured using the SFD.

Additionally, dose measurements were taken from the applicator surface using Gafchromic dosimetry film. This was achieved by wrapping an approximately 10.2 cm × 25.4 cm sized piece of film around the applicator before taking the measurements. Tape wrapped around the middle of the piece of film was used to secure the film firmly in place. The bottom edge of the film was approximately 12 mm above the distal end of the applicator. For the three film measurements, the shield configurations 90°, 180°, and 270° shielding were implemented and measured.

3.3 Data Processing

After obtaining measurement data, processing was implemented. Dose measurements were measured in coulomb (C), while calculations were done in gray, meaning that the measured doses required appropriate handling and conversion to units in which reliable comparisons could be conducted.

Converting the measurement doses from coulomb to gray was achieved post-measurement session, after calibration factors were obtained based on dosimetry film measurements. For this, the effective measurement point of each measurement detector was determined, and calibration factor deduced based on the dose measurements taken with film in that effective point. Additionally, background radiation and leakage radiation measured during the measurement session was subtracted from all dose measurements.

After subtraction of background radiation and radiation leakage and multiplying with the conversion factor, the results of dose measurements were rounded into the same accuracy as the original doses and the calculated doses using ROUND function on Microsoft® Excel® (Microsoft Corporation, Redmond, WA, USA).

At the end of the measurement session, measurements with dosimetry film were conducted as well, as per to the protocol described prior in this work. Approximately two days after the radiation of the films, they were scanned at STUK premises using Expression 12000XL A3 (Seiko Epson Corp., Suwa, Nagano, Japan) scanner. Protective pieces were placed on both sides of the films to prevent reflections. The dose measured from non-radiated films was 0.005 Gy, so there was no need to correct the doses on the radiated films.

Isodose images were created from the radiated films using a EBT3 reader software. Based on the film scans, percentages for dose profiles were obtained, as well. The doses for comparison with dose calculations were derived from the percentages by calculating the dose for each point based on the maximum recorded dose of the specific film and the percentage assigned to the point.

The data obtained from dose calculations and dose measurements was processed using MATLAB® (MathWorks, Natick, MA, USA). With MATLAB, dose curves and dose profiles were plotted.

4. RESULTS

The validation protocol specified by the manufacturer was produced for the purposes of this study. Based on this test procedure, it was deemed that the dose calculation program was successfully installed and working according to manufacturer specifications.

After validation in standard geometry, validation was conducted via dose calculations and measurements. As described earlier in this study, the validation protocol of Acuros BV was initiated with calibrations, in which air-kerma rates were calculated. Based on the specifications given by the manufacturer of the radiation source, the air-kerma rate calculated at the time of the measurements was 33.72 mGy/h.

Air-kerma rates obtained using well chambers were also calculated. For PTW well chamber, the calculated air-kerma rate was 33.53 mGy/h, while for HDR 1000 Plus well chamber, it was calculated as 33.74 mGy/h. The difference to air-kerma rate calculated using manufacturer specifications was -0.6% for PTW well chamber and 0.1% for HDR 1000 Plus well chamber.

Calibration factor for the conversion from Coulomb to Gray were obtained from dosimetry film. For the PTW the calibration factor was 0.99 Gy/nC, while it was 0.218 Gy/nC for the Razor, and 0.083 Gy/nC for the SFD. The radiation leaks measured and subtracted from the doses were 0.016 nC for PTW and 0.029 nC for Razor. For SFD, the leaks were 0.031 nC in 90° shielding, 0.033 nC in 180° shielding, and 0.034 nC in 270° shielding.

The validation protocol that was followed to conduct dose calculations and dose measurements was described earlier in this study. Based on this calculation and measurement data, dose curves were drawn with dose in gray as a function of distance in millimetres. These curves can be viewed in Figure 6.

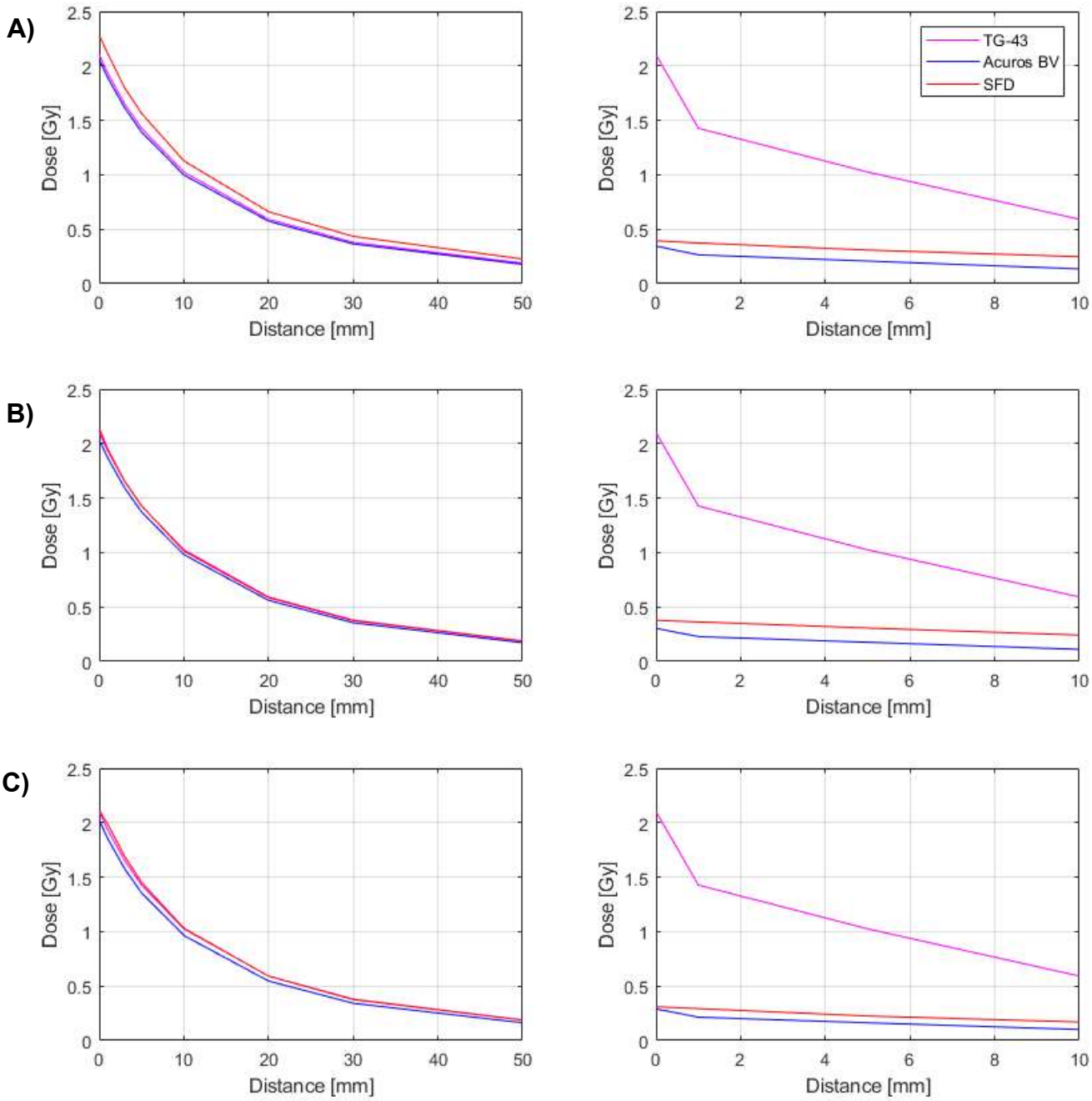

Figure 6. *Presented in this figure are the results of dose calculations and dose measurements. Location in millimetres on the x axis and dose in gray on the y axis. Dose curves are presented as function of distance of the reference point from the surface of the applicator, with unshielded points on the left column and shielded points on the right. Shield configurations on each row from top to bottom; A) 90°, B) 180°, and C) 270° shielded. In magenta is the dose calculated with TG-43 formalism, in blue the dose calculated with Acuros BV, and in red the dose measured using SFD.*

Differences between the two dose calculation algorithms can be studied quantitatively by executing a percentage error calculation between calculated doses and measured ones. This comparison can be seen in Table 3 for the mean percentage errors, as well as errors for 5 mm distance from applicator surface, given that this is a typical dose normalisation point.

Table 3. In the table, the mean percentage errors and percentage errors at 5 mm distance from applicator surface have been calculated when comparing Acuros BV and TG-43 to measured doses. The mean percentage error has been calculated for both shielded and unshielded sides of each applicator shielding.

	90° shielding		**180° shielding**		**270° shielding**	
	Un-shielded	**Shielded**	**Un-shielded**	**Shielded**	**Un-shielded**	**Shielded**
Acuros BV (mean)	-12.97%	-29.86%	-4.70%	-38.72%	-7.57%	-25.39%
Acuros BV (5 mm)	-11.00%	-32.69%	-4.06%	-42.67%	-6.68%	-27.56%
TG-43 (mean)	-10.27%	271.4%	0.23%	278.7%	-0.69%	392.2%
TG-43 (5 mm)	-8.76%	231.7%	-0.21%	233.9%	-1.72%	355.6%

Dose calculations were also done with Acuros BV and TG-43 in a plan without any applicators or shielding, to compare the difference between results produced by these two calculation methods. For dose calculations done on the surface of the applicator, the difference between the two algorithms was the Acuros BV estimating 1.16% lower dose. Similarly, Acuros BV calculated on average 1.28% lower dose for unshielded side and 1.01% lower dose for the shielded side of the applicator.

Given that dose measurements in 180° shielding configuration were conducted using two additional detectors, comparisons between the three different measurements devices can be drawn, as well. The curves drawn with dose as function of distance can be viewed in Figure 7.

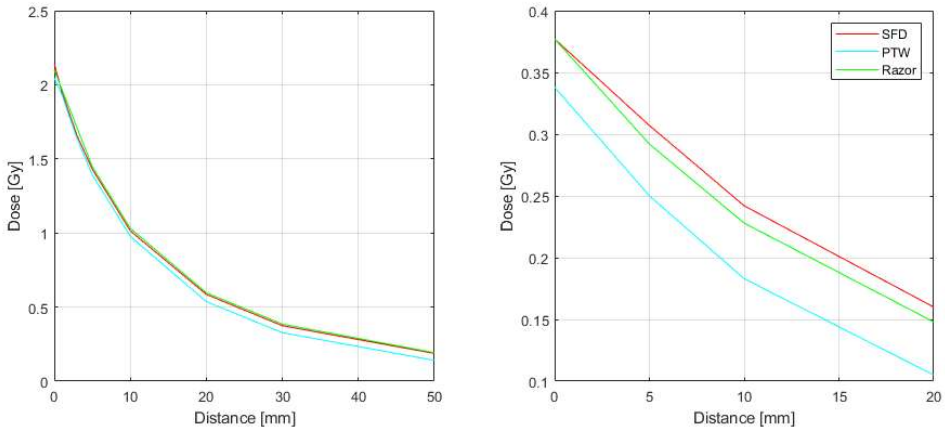

Figure 7. *Dose curves with dose measurements as function of distance using three different detectors. Unshielded points on left and shielded points on right. The SFD is presented in red, the PTW in cyan, and the Razor in green.*

Based on percentages obtained from the dosimetry film, dose profiles for each shield configuration could be plotted, as well. These profiles, along with profiles created with calculations implemented in similar geometry, can be viewed in Figure 8. The dose maxima estimated based on the film scans, which were used for the creation of these dose profiles were 2.38 Gy for the 90° shielded applicator, 2.39 Gy for the 180° shielded applicator, and 2.38 Gy for the 270° shielded applicator. For dose calculations, the maximum doses calculated with acuros were 2.06 Gy for the 90° shielded applicator, 2.03 Gy for the 180° shielded applicator, and 2.02 Gy for the 270° shielded applicator. With TG-43, the highest dose calculated for all these geometries was 2.11 Gy.

In Figure 9, presented are the scanned dosimetry films, with red indicating higher dose and blue indicating lower dose.

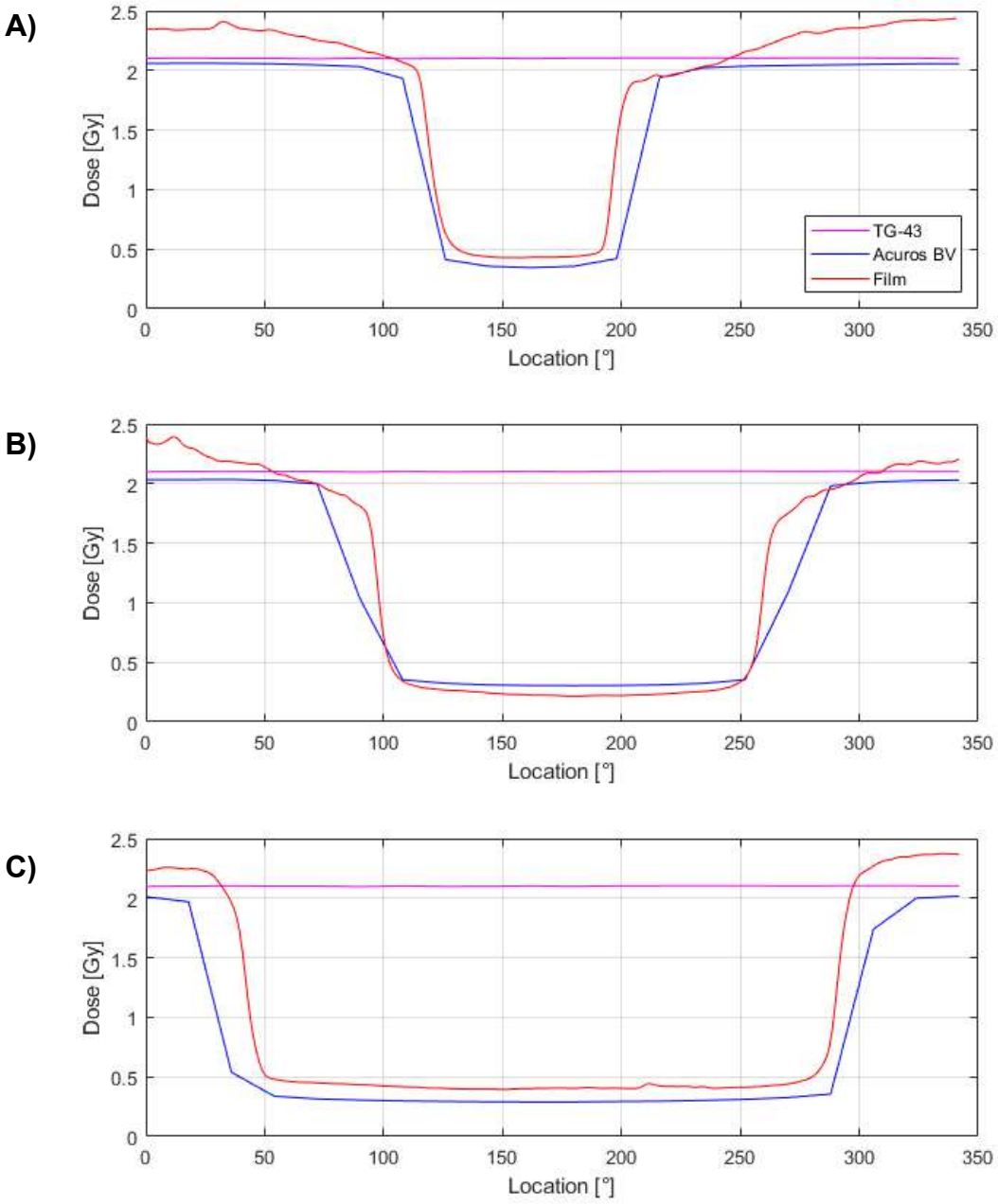

Figure 8. *Dose profiles for measurement and dose calculations. Location in degrees on the x axis and dose in gray on the y axis. From top to bottom; A) 90°, B) 180°, and C) 270° shielded applicator. The TG-43 displayed in magenta, Acuros BV in blue, and dosimetry film measurement in red.*

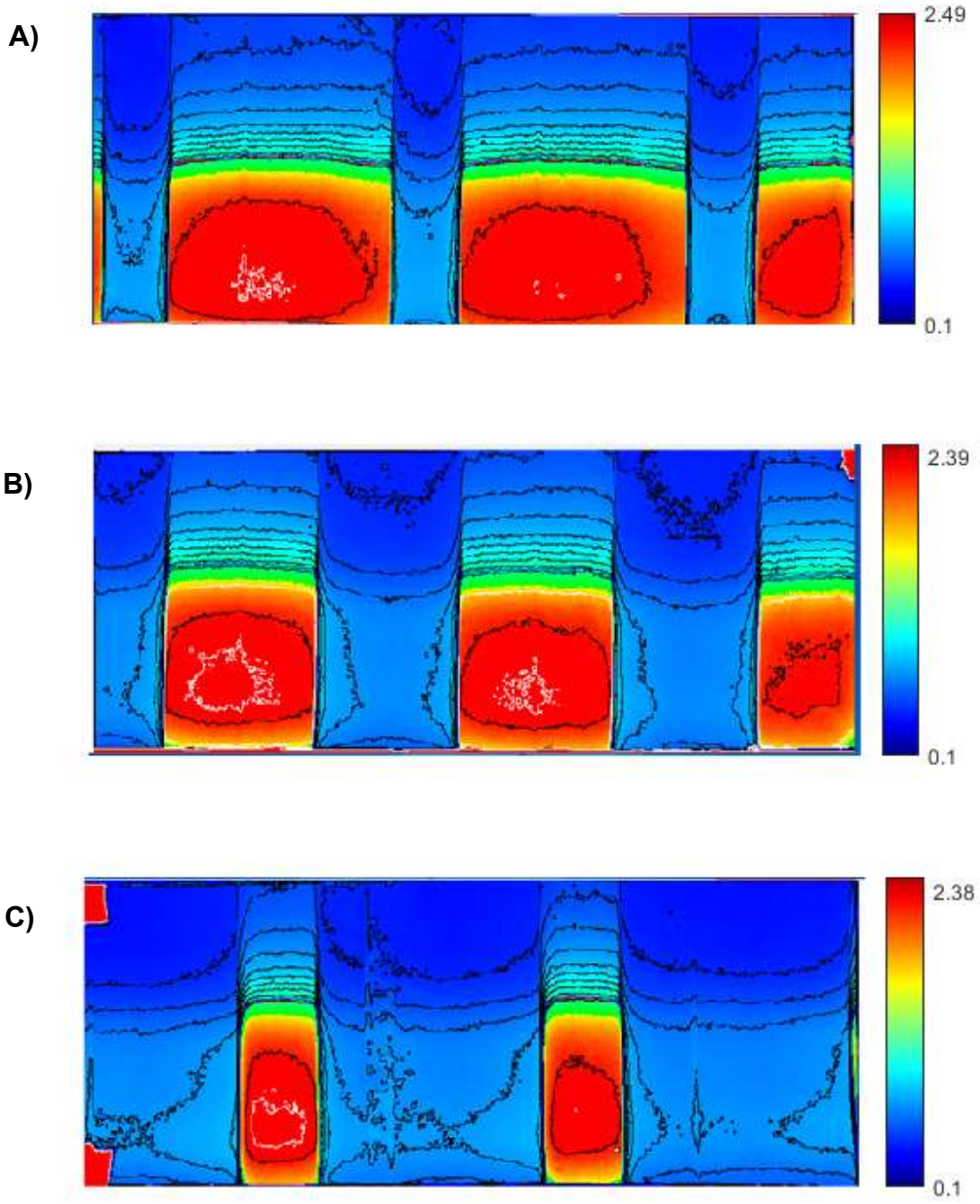

Figure 9. *Isodose curves based on dosimetry film measurements, doses expressed in gray. From top to bottom; A) 90° shielded applicator with dose range of [0.1 Gy, 2.49 Gy], B) 180° shielded with [0.1 Gy, 2.39 Gy], and C) 270° shielded with [0.1 Gy, 2.38 Gy]. In each image, areas where red is surrounded by a white line the dose is greatest, while in areas where dark blue is surrounded by a black line the dose is smallest. Original images courtesy of Petri Sipilä.*

5. DISCUSSION

The aim of this study was to investigate the Acuros BV radiation dose calculation algorithm and perform a quantitative and qualitative comparison of radiation doses obtained through dose calculations and dose measurements. The TG-43 formalism was also investigated in the same experiment setup. In addition, a literature review of relevant topics was conducted, as well.

Looking at the literature, the advantages of model-based dose calculation algorithms over factor-based ones seem noteworthy. The industry standard, the TG-43 formalism, whilst considered robust and reliable for most brachytherapy treatment-planning, has had its fair share of critique in the resent years when held in comparison to model-based dose calculation methods, such as the Monte Carlo methods, or Acuros BV. The absence of scatter conditions and the assumed homogeneity of the TG-43 formalism is what creates the most need for other methods for treatment-planning.

The model-based Acuros BV has previously been described as having accuracy comparable to Monte Carlo based dose calculation methods, while also working more efficiently than these methods. In this dissertation, the validation of Acuros BV, which is required for a novel treatment-planning algorithm before clinical implementation, was achieved. This validation was done in a standard geometry, as well as using a shielded applicator set designed for intracavitary HDR brachytherapy.

During the validation protocol, dose calculations obtained with Acuros BV and TG-43 were held in dosimetric comparison to the dose measured in same reference points. From Figure 6, it can be seen that the overall shape of the dose curves is quite similar between different calculation or measurement methods. Regardless, for the shielded side in all shielding geometries, the dose estimated by the TG-43 is considerably higher than the dose estimated by Acuros BV. For unshielded applicator geometries, both Acuros BV and TG-43 seem to estimate the radiation dose quite well.

When studying the mean percentage errors, it can be seen that the deviation from the measured dose is considerably higher on the shielded side than on the unshielded side of the applicator, similarly to visual estimation. This is particularly the case for doses calculated using the TG-43 formalism. This was to be expected, however, given that the TG-43 does not take shielding or applicator geometries into consideration in its working principle. Additionally, the error between dose calculations and dose measurements seems to grow the farther the reference point is from the applicator surface.

Interestingly, while performing poorly on the shielded side of the applicator, the TG-43 formalism estimates the doses to the unshielded side of the applicator with a smaller average percentage error than Acuros BV. The smallest average percentage error for both these algorithms is created on the unshielded side of the 180° shielded applicator.

When comparing these algorithms, it can be noticed that the TG-43 formalism tends to overestimate the dose, while Acuros BV tends to underestimate it. The TG-43 formalism typically performs within 2% accuracy of measured doses, or calculated doses with Monte Carlo methods [47]. With Monte Carlo dose calculation, accuracy of 1% can be achieved even in the near field of a HDR brachytherapy source [48].

For brachytherapy dose calculations, a suggested goal for accuracy is 3% at 5 mm distances [49]. However, in this study, the calculations and measurements of doses were conducted at distances of 15 mm from the source at minimum, given the diameter of the applicator. Additionally, this study was conducted on a shielded applicator, for which there seems to be no suggested goal for accuracy [49]. If we regardless study the errors at this distance from applicator surface, based on the results from Table 3, it can be seen that none of the results for Acuros BV are acceptable with this accuracy limit. For TG-43, only the errors calculated from the unshielded side of 180° shielded and 270° shielded geometries are beneath 3%.

The AAPM recommends brachytherapy dose delivery accuracy to remain between 5% and 10%, with the source calibration accuracy within 3% for LDR brachytherapy [50]. For HDR brachytherapy, the AAPM recommends creating a quality assurance program following the same recommendations for accuracy and safety as is recommended for LDR brachytherapy [51]. For these reasons, the estimation of accuracy of Acuros BV will be conducted using recommendations for LDR brachytherapy, as well.

As detailed earlier based on visual estimation of the dose curves, Acuros BV performs more accurately on the unshielded side than on the shielded side of the applicator. The percentage error for most reference points is beneath the limit of 10% when compared to measurements. All calculations for the unshielded side for 180° shielded applicator were between 5% and 10% deviation from the measured dose, while all but the calculation for last reference point at 50 mm distance from the applicator surface, were beneath 10% for the 270° shielding. For the 90° shielding, only the error for the dose calculated at the surface of the applicator was beneath 10%.

For the TG-43 formalism, the deviation of the dose calculation from dose measurement was considerably smaller on the unshielded side of the applicator. While the 90° shielding generated error within the recommended range of accuracy for reference points from

surface up to distance of 10 mm from surface, the rest of the error for other shielding configurations and reference points remained beneath 3%.

For the shielded side, neither of the algorithms produced results beneath 10% percentage error when compared to measurements, with the exception of dose calculated with Acuros BV at the surface of the applicator for 270° shielding. However, the differences between these two algorithms are even more pronounced on the shielded side. Acuros BV underestimating the dose by 29.86% for 90° shielding, by 38.72% for 180° shielding, and by 25.39% for 270° shielding, on average. On the other hand, TG-43 formalism overestimates the dose by 271.4% for 90° shielding, by 278.7% for 180° shielding, and by 392.2% for 270° shielding, on average. This is a considerable difference, which should be taken into account during treatment-planning. These percentages and their computation method can be studied further in Appendix A.

Additionally, error was calculated during source calibration. Both error calculations resulted in values within acceptable limits.

If we study Figure 7, which presents us the three detectors used in measurement, it is evident that the dose measured by the PTW is lower than what was measured by the SFD, or the Razor, for that matter. After calibration, doses for the PTW could be obtained based on the conversion factor. When compared to values obtained from dosimetry film in the same point, it was noticed that the PTW gave the most accurate result, followed by the SFD and the Razor, in that order. Based on these observations, we can speculate that the dose measured by the SFD may be greater than the true dose, indicating that the mean errors shown by Acuros BV could in turn be smaller. However, this would have to be proven in a further study.

Dose profiles were also created for the purposes of this study. When comparing dose profiles created with dose calculations against dose profiles based on dosimetry film scans, it must be noted, that precise comparison of dose values is not possible when studying the results presented in Figure 8. This is since the profiles based on dosimetry film were plotted based on the percentages obtained from the film scans and the maximum values measured on the films. This affects the scaling of the dose profiles and the overall values of the doses, meaning that individual values for doses are not correctly presented in the profiles.

For instance, the estimated minimum value of the curves appears smaller on the profiles, than what was estimated previously. Additionally, the film was wrapped around the applicator, overlapping at some parts, meaning that the doses could not be recorded uniformly across the surface, but rather with slight variance to the location of each point.

Another aspect affecting the reliability of the dosimetry film measurements is the leakage radiation, which can be witnessed in Figure 9, represented in red at the corners and sides of the isodose images. An artefact can be seen in the isodose curve for 270° shielded applicator, as well.

However, the overall shapes of the dose profiles are still reliable and usable for comparison with dose profile calculations. We can, for instance, see the slightly greater and less defined dose on the unshielded areas of the applicator, as well as the less sloped and gentle curve when dose decreases over the shielding material, and then increases outside it, when compared to Acuros BV. As expected, the TG-43 formalism does not take the shielding into account in its dose calculation.

Retrospectively, it can be said that this study could have benefited from repetition of dose measurements and dose calculations for increased accuracy and precision. Similarly, this validation protocol was only implemented using one applicator of the possible five included in the shielded applicator set. This, however, is acceptable, since the size and diameter of the quarter pieces used for shielding remains the same for each applicator, i.e., only the thickness of the surrounding acrylic applicator is altered when switching between different applicators. The accuracy of the study could have been improved with a more reliable method of dose profile construction of dosimetry film measurements, as well, given that this method is a very accurate dose measurement technique.

By repetition of the experiment, error sources noticed during dose calculations and measurements could also be observed and addressed more in depth. For the measurement session conducted for this study, however, error could have been caused by imprecisely set applicators and the shielding materials within, which were rotated and set by hand. Measurements were also taken by moving the detector on the stand by hand, which could disturb the experiment setup or cause minor differences to results.

During dose calculations, reference points were likewise set by hand, although they could later on be corrected by inputting precise values into the treatment-planning system. Applicators and shielding were still set by hand, and the isodose curves visually estimated and corrected when creating the treatment plan.

Other limitations of this study include the use of a water phantom, meaning that doses and dose distributions were not studied in tissue. Water is merely a representation for tissue and does not account for heterogeneities or anatomies present in tissue. Even though the pelvic area is quite water equivalent, in this study the effect of tissue was completely ignored.

Additional sources of error for this study can be found in data processing, where results were rounded or converted from one unit to another using different conversion factors. Human error when recording doses during measurement session, as well as later on when copying calculated and measured doses between different programs and software, cannot be ignored, either.

It is important to take into account these limitations and characteristics of the Acuros BV algorithm and this validation protocol, given the inherent risks of HDR brachytherapy. When implementing HDR brachytherapy, doses to target, as well as surrounding tissues and organs at risk, is much greater than in LDR, and this should be considered in the assessment of treatment plan accuracy. In treatment-planning, risks may arise for instance from inaccuracies in dwell times and dwell positions, or from image reconstruction when using 3-dimensional imaging techniques. Possibility for human error is present in many phases of the treatment, beginning at diagnosis and the imaging of the patient, to the creation of the treatment plan and its implementation with the use of applicators and other relevant machinery. Error in dose calculation is only one part of the cumulative inaccuracy that is generated throughout the whole treatment regarding individual patients.

An update on the estimation of Acuros BV accuracy using the results of this study could be conducted when guidelines for shielded applicator and HDR brachytherapy are defined better. The need for additional research on brachytherapy source calibration and dose delivery accuracy has been acknowledged by the AAPM, as well [52].

While retaining significant inaccuracy, the Acuros BV algorithm for gynecological HDR brachytherapy still holds much promise. In recent years, Acuros BV has garnered much attention, leading to reports on validations for its use in HDR brachytherapy. Similarly to this study, it has been reported that the TG-43 estimates higher doses than Acuros BV [54]. The overall accuracy of Acuros BV has been reported in these studies, as well. Validation has also been performed in a quite similar setting, for HDR brachytherapy with a shielded cylinder applicator, where high accuracy for Acuros BV was achieved [55]. Given that the topic is relatively recent, other studies regarding Acuros BV validation have been conducted but not yet peer-reviewed, also.

As discussed, shielded applicators combined with a dose calculation algorithm that takes into account inhomogeneities and scatter conditions has a potential to be implemented for a more individualised brachytherapy treatment for certain patients, while reducing dose to organs at risk, toxicity, and other side effects. While the application areas for

these specific applicators are quite slim, quantifiable knowledge on the accuracy of Acuros BV is regardless significant for clinical use. Given that Acuros BV can be utilised for other brachytherapy treatments as well, it is important to have data on its overall accuracy.

Within the boundaries of our experiment setup and methodology, the research questions to this dissertation have been answered; Acuros BV does estimate the does quite well, mostly within the AAPM recommended accuracy between 5% and 10%, but only for the 180° shielding and 270° on the unshielded side of the applicator. If this methodology is implemented during HDR brachytherapy treatment, the underestimation of doses needs to be addressed somehow. For the implementation of the 90° shielding geometry, this measure is critical, given the greater error associated with this shield configuration. For the unshielded side, the TG-43 formalism seems to perform better on average, but grossly worse for the shielded side, as it typically overestimates the dose.

With these aspects in mind, the use of Acuros BV is recommended for gynaecological HDR brachytherapy treatments when using this specific applicator set, given the overall greater accuracy over the TG-43 formalism in this particular setting. The underestimation of dose, particularly for the shielded side of the applicator, that was reported in this study, however, needs to be addressed. A correction factor that recognises the underestimation of dose is suggested to be applied during treatment-planning and implementation.

.

6. CONCLUSIONS

In this study, the validation protocol for Acuros BV was implemented. Dose calculations and dose measurements with similar reference points and applicator shielding geometries were conducted, using both Acuros BV and the TG-43 formalism for dose calculations. It was found that Acuros BV slightly underestimates the dose when compared to measured dose, more so on the shielded side of the applicator. Acuros BV performed mostly within 10% inaccuracy limit for 180° shielding and 270° shielding configurations on the unshielded side of the applicator, while producing more error for the 90° shielding geometry, and all geometries on the shielded side of the applicator. The TG-43 formalism, on the other hand, slightly overestimates dose, significantly so, when studying the shielded side of the applicator.

Dose profiles plotted based on dosimetry film were also obtained. The overall shape of these profiles tells us that Acuros BV estimates the dose quite well but retains a less drastic slope when dose decreases or increases around the shielded portion of the applicator when compared to dosimetry film.

With the validation of Acuros BV algorithm for a shielded applicator set, HDR brachytherapy treatments may be implemented using the algorithm and the applicator set used for the validation protocol of this study. The validation also gives us information on the overall accuracy of the algorithm, so the benefits of its use can be considered for other application areas, as well. Potential benefits for use of this algorithm combined with shielded applicators are mostly patient-centred.

However, given the noteworthy underestimation of dose exhibited by Acuros BV, particularly on the shielded side of the applicator, a method of compensation that acknowledges this needs to be implemented. This method could be a correction factor, for instance. The results of this study could also be updated when there are more defined guidelines available for inaccuracy limits for HDR brachytherapy for shielded applicators.

REFERENCES

[1] H. Sung, J. Ferlay, R. L. Siegel, M. Laversanne, I. Soerjomataram, A. Jemal, and F. Bray, “Global cancer statistics 2020: GLOBOCAN estimates of incidence and mortality worldwide for 36 cancers in 185 Countries,” *CA: A Cancer Journal for Clinicians*, vol. 71, pp. 209–249, 2021, doi: 10.3322/caac.21660.

[2] P. M. Devlin, G. N. Cohen, and S. L. Wolden, *Brachytherapy: Applications and Techniques*, 2nd ed. New York: Demos Medical, 2016.

[3] K. A. Bergström, R. Härkönen, K. Kairemo, S-L. Karonen, J. Knuuti, J. T. Kuikka, B-A Lamberg, E. Länsimies, K. Liewendahl, P. Nikkinen, A. Rekonen, S. Savolainen, E. Vannien, E. Vauramo, and U. Wegelius, “The development of nuclear medicine in Finland: A review on the occasion of the 40th anniversary of the Finnish Society of Nuclear Medicine,” *Clinical Physiology*, vol. 20, pp. 317–329, 2000, doi: 10.1046/j.1365-2281.2000.00267.x.

[4] J. Nicholas Lukens, M. Gamez, K. Hu, and L. B. Harrison, “Modern brachytherapy,” *Seminars in Oncology*, vol. 41, pp. 831–847, 2014, doi: 10.1053/J.SEMINONCOL.2014.09.015.

[5] J. N. Aronowitz, “Afterloading: the technique that rescued brachytherapy,” *International Journal of Radiation Oncology, Biology, Physics*, vol. 92, pp. 479–487, 2015, doi: 10.1016/J.IJROBP.2015.02.014.

[6] S. Otter, A. Franklin, M. Ajaz, and A. Stewart, “Improving the efficiency of image guided brachytherapy in cervical cancer,” *Journal of Contemporary Brachytherapy*, vol. 8, pp. 557–565, 2016, doi: 10.5114/jcb.2016.64452.

[7] J. Skowronek, “Pulsed dose rate brachytherapy: is it the right way?” *Journal of Contemporary Brachytherapy*, vol. 2, p. 107–113, 2010, doi: 10.5114/JCB.2010.16921.

[8] J. P. Gibbons, *Khan’s The Physics of Radiation Therapy*, 6th ed. Philadelphia: Wolters Kluwer Health, 2020. doi: 10.4103/jmp.jmp_17_20.

[9] U. Mahantshetty, G. Lavanya, S. Grover, C. . Akinfenwa, H. Carvalho, and N. Amornwichet, “Incidence, treatment and outcomes of cervical cancer in low- and middle-income countries,” *Clinical Oncology*, vol. 33, pp. e363–e371, 2021, doi: 10.1016/j.clon.2021.07.001.

[10] C. Marth, F. Landoni, S. Mahner, M. McCormack, A. Gonzales-Martin, and N.

Colombo, “Cervical cancer: ESMO clinical practice guidelines for diagnosis, treatment and follow-up,” *Annals of Oncology*, vol. 28, pp. iv72–iv83, 2017, doi: 10.1093/annonc/mdx220.

[11] N. Colombo, E. Preti, F. Landoni, S. Carinelli, A. Colombo, C. Marini, and C. Sessa, “Endometrial cancer: ESMO clinical practice guidelines for diagnosis, treatment and follow-up,” *Annals of Oncology*, vol. 24, pp. vi33–vi38, 2013, doi: 10.1093/ANNONC/MDT353.

[12] E. K. K. Tanderup, I. El Naqa, and D. Carlson, “Advances in image-guided brachytherapy,” *International Journal of Radiation Oncology, Biology, Physics*, vol. 97, no. 5, pp. 873–875, Apr. 2017, doi: 10.1016/J.IJROBP.2017.01.013.

[13] C. Chargari, E. Deutsch, P. Blanchard, S. Gouy, H. Martelli, F. Guérin, I. Dumas, A. Bossi, P. Morice, A. N. Viswanathan, and C. Haie-Meder, “Brachytherapy: an overview for clinicians,” *CA: A Cancer Journal for Clinicians*, vol. 69, pp. 386–401, 2019, doi: 10.3322/caac.21578.

[14] S. Sabater, I. Andres, V. Lopez-Honrubia, R. Berenguer, M. Sevillano, E. Jimenez-Jimenez, A. Rovirosa, and M. Arenas, “Vaginal cuff brachytherapy in endometrial cancer: a technically easy treatment?” *Cancer Management and Research*, vol. 9, p. 351–362, 2017, doi: 10.2147/CMAR.S119125.

[15] J. Lian, G. Dundas, M. Carlone, S. Ghosh, and R. Pearcey, “Twenty-year review of radiotherapy for vaginal cancer: an institutional experience,” *Gynecologic Oncology*, vol. 111, pp. 298–306, 2008, doi: 10.1016/j.ygyno.2008.07.007.

[16] H. Kim, M. S. Rajagopalan, C. Houser, and S. Beriwal, “Dosimetric comparison of multichannel with one single-channel vaginal cylinder for vaginal cancer treatments with high-dose-rate brachytherapy,” *Brachytherapy*, vol. 13, pp. 263–267, 2014, doi: 10.1016/j.brachy.2013.08.009.

[17] M. Korkmaz, M. K. Eryikmaz, Ü. Kerimoğlu, M. Karaağaç, A. Demirkıran, E. T. Demir, and M. Artaç, “Vaginal metastasis in solid tumours: our four cases and review of the literature,” *Journal of the Egyptian National Cancer Institute*, vol. 33, pp. 1–6, 2021, doi: 10.1186/s43046-021-00058-4.

[18] S. S. Patankar, A. I. Tergas, I. Deutsch, W. M. Burke, J. Y. Hou, C. V. Ananth, Y. Huang, A. I. Neugut, D. L. Hershman, and J. D. Wright, “High versus low-dose rate brachytherapy for cervical cancer,” *Gynecologic Oncology*, vol. 136, p. 534–542, 2015, doi: 10.1016/J.YGYNO.2014.12.038.

[19] G. A. Viani, G. B. Manta, E. J. Stefano, and L. I. de Fendi, “Brachytherapy for

cervix cancer: low-dose rate or high-dose rate brachytherapy: a meta-analysis of clinical trials," *Journal of Experimental & Clinical Cancer Research*, vol. 28, pp. 1–12, 2009, doi: 10.1186/1756-9966-28-47.

[20] R. Autorino, L. Tagliaferri, M. Campitelli, D. Smaniotto, A. Nardangeli, G. C. Mattiucci, G. Macchia, B. Gui, M. Miccò, F. Mascilini, G. Ferrandina, G. Kovacs, V. Valentini, and M. A, Gambacorta, "EROS study: evaluation between high-dose-rate and low-dose-rate vaginal interventional radiotherapy (brachytherapy) in terms of overall survival and rate of stenosis," *Journal of Contemporary Brachytherapy*, vol. 10, p. 315–320, 2018, doi: 10.5114/JCB.2018.77953.

[21] R. Pötter, K. Tanderup, C. Kirisits, A. de Leeuw, K. Kirchheiner, R. Nout, L. T. Tan, C. Haie-Meder, U. Mahantshetty, B. Segeding, P. Hoskin, K. Bruheim, B. Rai, F. Huang, E. Van Limbergen, M. Schmid, N. Nesvacil, A. Sturdza, L. Fokdal, N. B. K. Jensen, D. Georg, M. Assenholt, Y. Seppenwoolde, C. Nomden, I. Fortin, S. Chopra, U. van der Heide, T. Rumpold, J. C. Lindegaard and I. Jürgenliemk-Schulz, "The EMBRACE II study: the outcome and prospect of two decades of evolution within the GEC-ESTRO GYN working group and the EMBRACE studies," *Clinical and Translational Radiation Oncology*, vol. 9, pp. 48–60, 2018, doi: 10.1016/j.ctro.2018.01.001.

[22] D. M. Narasimhulu. A. Cope, I. B. Riaz, I. Petersen, W. Cilby, C. Langstraat, G. Glaser, A. Kumar, S. Cappuccio, H. Murad, C. West, and A. Mariani, "External beam radiotherapy versus vaginal brachytherapy in patients with stage II endometrial cancer: a systematic review and meta-analysis," *International Journal of Gynecological Cancer*, vol. 30, pp. 1–9, 2020. doi: 10.1136/ijgc-2020-001199.

[23] K. Derks, J. L. G. Steenhuijsen, H. A. Van Den Berg, S. Houterman, J. Cnossen, P. Van Haaren, and K. De Jaeger, "Impact of brachytherapy technique (2D versus 3D) on outcome following radiotherapy of cervical cancer," *Journal of Contemporary Brachytherapy*, vol. 10, pp. 17–25, 2018, doi: 10.5114/jcb.2018.73955.

[24] F. A. Hashemi, S. Mansouri, M. Aghili, E. Esmati, M. Babei, A. Saeedian, S. Moalej, and R. Jaberi, "A comparison between 2D and 3D planning of high-dose-rate vaginal cuff brachytherapy in patients with stage I-II endometrial cancer using cobalt-60," *Journal of Contemporary Brachytherapy*, vol. 13, pp. 526–532, 2021, doi: 10.5114/jcb.2021.110312.

[25] S. R. Palled, N. K. Radhakrishna, S. Manikantan, H. Khanum, B. K. Venugopal, and L. Vishwanath, "Dosimetric comparison of manual forward planning with

uniform dwell times versus volume-based inverse planning in interstitial brachytherapy of cervical malignancies," *Reports of Practical Oncology and Radiotherapy*, vol. 25, pp. 851–855, 2020, doi: 10.1016/j.rpor.2020.08.005.

[26] E. Lessard, I. C. Hsu, and J. Pouliot, "Inverse planning for interstitial gynecologic template brachytherapy: truly anatomy-based planning," *International Journal of Radiation Oncology, Biology, Physics*, vol. 54, pp. 1243–1251, 2002, doi: 10.1016/S0360-3016(02)03802-6.

[27] Y. A. Bahadur, C. Constantinescu, A. H. Hassouna, M. M. Eltaher, N. M. Ghassal, and N. A. Awad, "Single versus multichannel applicator in high-dose-rate vaginal brachytherapy optimized by inverse treatment planning," *Journal of Contemporary Brachytherapy*, vol. 6, p. 362–369, 2015, doi: 10.5114/JCB.2014.47816.

[28] M. Carrara, D. Cusumano, T. Giandini, C. Tenconi, E. Mazzarella, S. Grisotto, E. Massari, D. Mazzeo, A. Cerrotta, B. Pappalardi, C. Fallai, and E. Pignoli, "Comparison of different treatment planning optimization methods for vaginal HDR brachytherapy with multichannel applicators: a reduction of the high doses to the vaginal mucosa is possible," *Physica Medica*, vol. 44, pp. 58–65, 2017, doi: 10.1016/j.ejmp.2017.11.007.

[29] H.-G. Menzel, "ICRU report 91: prescribing, recording, and reporting of stereotactic treatments with small photon beams," *Journal of the International Commission on Radiation Units and Measurements*, vol. 14, pp. 65–75, 2014, doi: 10.1093/JICRU/NDX014.

[30] K. Asnaashari, M. R. G. Nodehi, S. R. Mahdavi, S. Gholami, and H. R. Khosravi, "Dosimetric comparison of different inhomogeneity correction algorithms for external photon beam dose calculations," *Journal of Medical Physics*, vol. 38, pp. 74–81, 2013, doi: 10.4103/0971-6203.111310.

[31] N. Papanikolaou and S. Stathakis, "Dose-calculation algorithms in the context of inhomogeneity corrections for high energy photon beams," *Medical Physics*, vol. 36, pp. 4765-4775, 2009, doi: 10.1118/1.3213523.

[32] E. Poon and F. Verhaegen, "A CT-based analytical dose calculation method for HDR 192^{Ir} brachytherapy," *Medical Physics*, vol. 36, pp. 4765–4775, 2009, doi: 10.1118/1.3184695.

[33] K. Zourari, E. Pantelis, A. Moutsatsos, L. Sakelliou, E. Georgiou, P. Karaiskos, and P. Papagiannis, "Dosimetric accuracy of a deterministic radiation transport based 192^{Ir} brachytherapy treatment planning system. Part III. Comparison to

Monte Carlo simulation in voxelized anatomical computational models," *Medical Physics*, vol. 40, pp. 1–9, 2013, doi: 10.1118/1.4770275.

[34] M. J. Rivard, B. M. Coursey, W. F. Hanson, M. Saiful Huq, G. S. Ibbott, M. G. Mitch, R. Nath, and J. F. Williamson, "Update of AAPM Task Group No. 43 report: a revised AAPM protocol for brachytherapy dose calculations," *Medical Physics*, vol. 31, pp. 633–674, 2004. doi: 10.1118/1.1646040.

[35] J. K. Mikell, A. H. Klopp, M. Price, and F. Mourtada, "Commissioning of a grid-based Boltzmann solver for cervical cancer brachytherapy treatment planning with shielded colpostats," *Brachytherapy*, vol. 12, pp. 645–653, 2013, doi: 10.1016/J.BRACHY.2013.04.007.

[36] G. Famulari, M. A. Renaud, C. M. Poole, M. D. C. Evans, J. Seuntjens, and S. A. Enger, "RapidBrachyMCTPS: a Monte Carlo-based treatment planning system for brachytherapy applications," *Physics in Medicine and Biology*, vol. 63, pp. 1–13, 2018, doi: 10.1088/1361-6560/aad97a.

[37] P. Andreo, "Monte Carlo simulations in radiotherapy dosimetry," *Radiation Oncology*, vol. 13, pp. 1–15, 2018, doi: 10.1186/s13014-018-1065-3.

[38] M. W. K. Kan, P. K. N. Yu, and L. H. T. Leung, "A review on the use of grid-based Boltzmann equation solvers for dose calculation in external photon beam treatment planning," *BioMed Research International*, vol. 1, pp. 1–10, 2013, doi: 10.1155/2013/692874.

[39] M. Sinnatamby, V. Nagarajan, S. Reddy, G. Karunanidhi, and V. Singhavajala, "Dosimetric comparison of Acuros™ BV with AAPM TG43 dose calculation formalism in breast interstitial high-dose-rate brachytherapy with the use of metal catheters," *Journal of Contemporary Brachytherapy*, vol. 7, pp. 273–279, 2015, doi: 10.5114/jcb.2015.54052.

[40] A. Naseri and A. Mesbahi, "Application of Monte Carlo calculations for validation of a treatment planning system in high dose rate brachytherapy," *Reports of Practical Oncology and Radiotherapy*, vol. 14, pp. 200–204, 2009, doi: 10.1016/j.rpor.2009.12.003.

[41] Z. Tian, M. Zhang, B. Hrycushko, K. Albuquerque, S. B. Jiang, and X. Jia, "Monte Carlo dose calculations for high-dose-rate brachytherapy using GPU-accelerated processing," *Brachytherapy*, vol. 15, pp. 387–398, 2016, doi: 10.1016/j.brachy.2016.01.006.

[42] A. Fogliata, G. Nicolini, A. Clivio, E. Vanetti, P. Mancosu, and L. Cozzi, "Dosimetric

validation of the Acuros XB Advanced Dose Calculation algorithm: fundamental characterization in water," *Physics in Medicine and Biology*, vol. 56, pp. 1879–1904, 2011, doi: 10.1088/0031-9155/56/6/022.

[43] R. Seppänen, L. Mannila, M. Kervinen, I. Parkkila, P. Konttinen, L. Karkela, and T. Yli-Kokko, *MAOL-taulukot*, 1st ed. Keuruu: Otava, 2013.

[44] N. F. S. Nor Azmi, A. Zakaria, R. Abdullah, and N. Abdul Hadi, "Comparison QA methods of brachytherapy using well ionization chamber and in-air method," *Malaysian Journal of Fundamental and Applied Sciences*, vol. 8, pp. 246–252, 2012, doi: 10.11113/mjfas.v8n4.152.

[45] S. B. Gursel, A. Serarslan, A. D. Meydan, N. Okumus, and T. Yasayacak, "A comparison of tandem ring and tandem ovoid treatment as a curative brachytherapy component for cervical cancer," *Journal of Contemporary Brachytherapy*, vol. 12, pp. 111–117, 2020, doi: 10.5114/jcb.2020.94308.

[46] G. Lymperopoulou, E. Pantelis, P. Papagiannis, H. Rozaki-Mavrouli, L. Sakelliou, D. Baltas, and P. Karaiskos, "A Monte Carlo dosimetry study of vaginal 192^{Ir} brachytherapy applications with a shielded cylindrical applicator set," *Medical Physics*, vol. 31, pp. 3080–3086, 2004, doi: 10.1118/1.1810233.

[47] A. Palmer, D. Bradley, and A. Nisbet, "Physics-aspects of dose accuracy in high dose rate (HDR) brachytherapy: source dosimetry, treatment planning, equipment performance and in vivo verification techniques," *Journal of Contemporary Brachytherapy*, vol. 4, pp. 81–91, 2012. doi: 10.5114/jcb.2012.29364.

[48] T. Wong, S. Wallace, W. Fernando, W. Schumer, and G. Quong, "Dose errors in the near field of an HDR brachytherapy stepping source," *Physics in Medicine and Biology*, vol. 44, pp. 357–363, 1999, doi: 10.1088/0031-9155/44/2/005.

[49] J. Van Dyk, R. B. Barnett, J. E. Cygler, and P. C. Shragge, "Commissioning and quality assurance of treatment planning computers," *International Journal of Radiation Oncology, Biology, Physics*, vol. 26, pp. 261–273, 1993, doi: 10.1016/0360-3016(93)90206-B.

[50] R. Nath, L. L. Anderson, J. A. Meli, A. J. Olch, J. A. Stitt, and J. F. Williamson, "Code of practice for brachytherapy physics: report of the AAPM radiation therapy committee task group no. 56," *Medical Physics*, vol. 24, pp. 1557–1598, 1997. doi: 10.1118/1.597966.

[51] H. D. Kubo, G. P. Glasgow, T. D. Pethel, B. R. Thomadsen, and J. F. Williamson, "High dose-rate brachytherapy treatment delivery: report of the AAPM Radiation

Therapy Committee Task Group No. 59," *Medical Physics*, vol. 25, pp. 375–403, 1998, doi: 10.1118/1.598232.

[52] L. A. DeWerd, G. S. Ibbott, A. S. Meigooni, M. G. Mitch, M. J. Rivard, K. E. Stump, B. R. Thomadsen, and J. L. M. Venselaar, "A dosimetric uncertainty analysis for photon-emitting brachytherapy sources: report of AAPM Task Group nN. 138 and GEC-ESTRO," *Medical Physics*, vol. 38, pp. 762–801, 2011, doi: 10.1118/1.3533720.

[53] A. Dagli, F. Yurt, and G. Yegin, "Evaluation of BrachyDose Monte Carlo code for HDR brachytherapy: dose comparison against Acuros®BV and TG-43 algorithms," *Journal of Radiotherapy in Practice*, vol. 19, pp. 1–8, 2020, doi: 10.1017/S1460396919000220.

[54] Y. Li, Z. Tian, B. Hrycushko, S. Jiang, and X. Jia, "SU-E-T-795: validations of dose calculation accuracy of Acuros BV in high-dose-rate (HDR) brachytherapy with a shielded cylinder applicator using Monte Carlo simulation," *Medical Physics*, vol. 42, pp. 3520, 2015, doi: 10.1118/1.4925159.

APPENDIX A: PERCENTAGE ERRORS

The differences between dose calculations and dose measurements were calculated using the formula for percentage error

$$Percentage\ Error\ = \frac{Estimated\ Number - \ Actual\ Number}{Actual\ number} \times 100, \qquad (12)$$

based on which the amount of error as well as the direction of the deviation from measurement dose could be concluded. The results for this comparison for Acuros BV and the TG-43 formalism can be viewed in Table 4, with the exception of dose at 1 mm distance from applicator surface at 180° shielding, since there was no measurement data for this point.

Table 4. Percentage errors for reference points on unshielded and shielded sides of the applicator. Results in percentages and from top to bottom; at distances 0, 1, 3, 5, 10, 20, 30, 50 mm from applicator surface for unshielded side, and at 0, 1, 5 and 10 mm for shielded side. Means from top to bottom; unshielded and shielded. To results missing for 180° shielded applicator at 1 mm distance from surface. Results are rounded.

	Acuros BV			**TG-43**		
	90°	180°	270°	90°	180°	270°
Unshielded	-9.66	-5.09	-4.49	-7.73	-1.87	-0.61
	-10.5	-4.20	-6.69	-8.56	-0.87	-2.67
	-10.2	-3.80	-6.74	-8.12	-0.18	-2.25
	-11.0	-4.06	-6.68	-8.76	-0.21	-1.72
	-11.5	-3.25	-6.50	-9.13	1.08	-0.58
	-13.2	-4.10	-7.61	-10.4	1.20	0.17
	-16.1	-5.08	-9.04	-12.6	1.60	1.06
	-21.6	-8.02	-12.8	-16.7	1.07	1.07
Shielded	-12.4	-19.4	-6.45	433.5	457.6	578.0
	-29.1		-27.0	281.6		387.0
	-32.7	-42.7	-27.6	231.7	233.9	355.6
	-45.2	-54.1	-40.6	138.7	144.6	248.2
Mean	-12.97	-4.70	-7.57	-10.3	0.23	-0.69
	-29.9	-38.7	-25.4	271.4	278.7	392.2